EFFECTS OF DISCHARGE AND MORPHOLOGY ON FLUVIAL SOUND

by

Scott J. Gauvain

A thesis

submitted in partial fulfillment

of the requirements for the degree of

Master of Science in Geophysics

Boise State University

August 2023

BOISE STATE UNIVERSITY GRADUATE COLLEGE

DEFENSE COMMITTEE AND FINAL READING APPROVALS

of the thesis submitted by

Scott J. Gauvain

Thesis Title: Effects of Discharge and Morphology on Fluvial Sound

Date of Final Oral Examination: April 28, 2023

The following individuals read and discussed the thesis submitted by student Scott J. Gauvain, and they evaluated his presentation and response to questions during the final oral examination. They found that the student passed the final oral examination.

Jacob Anderson, Ph.D.	Chair, Supervisory Committee
James McNamara, Ph.D.	Member, Supervisory Committee
Elowyn Yager, Ph.D.	Member, Supervisory Committee

The final reading approval of the thesis was granted by Jacob Anderson, Ph.D., Chair of the Supervisory Committee. The thesis was approved by the Graduate College.

DEDICATION

I would first like to dedicate this thesis to my grandmother, Gerri Gauvain, and my Aunt, Karen Gauvain, both of whom my family lost this past year. Your examples of grace and strength have enabled me to be who I am today. I would also like to dedicate this work to my parents, Steve and Terri Gauvain, whose love and support have carried me through life and this degree. Finally, to my three siblings, especially Ben Gauvain, who encouraged me to study physics and to follow my dreams. Additionally, thank you to my friends and colleagues for the priceless shared experiences and discussions.

ACKNOWLEDGMENTS

This work was funded by NSF award EAR-2051670 and the Burnham student grant from the Boise State Department of Geosciences. I would like to acknowledge committee members Elowyn Yager and James McNamara for their invaluable guidance on this thesis. I would also like to acknowledge individuals who helped collect acoustic and discharge data, including: The University of Idaho Streamlab, N. Ashmead, P. Aish-lin-Cedillo, B. Rosenblatt, T. Tatum, A. Bosa, M. Holahan, O. Walsh, B. Basham, T. Beschorner, M. Beers, and J. Johnson.

ABSTRACT

Rivers, streams, and tributaries play a critical role in the global water cycle and their dispersion of freshwater is essential for widespread human consumption, crop irrigation, and hydropower generation. Currently, there is a need for innovative, non-invasive, and low-cost methods of surface freshwater discharge gauging. With careful site selection, recording the acoustics produced by streamflow could be used reliably and inexpensively to infer changes in local discharge. An important knowledge gap currently preventing the use of acoustics for stream gauging is the unknown relationships by which stream sounds depend on discharge and stream morphology. To address this, I record and characterize sound and infrasound produced by morphologically unique features of the Boise River and Dry Creek in Southern Idaho across multi-year spans. Using a flume and a custom-made adjustable plunge-pool apparatus, I record acoustics produced by plunge-pool flow conditions at several scales of discharge and morphology to understand how channel and flow structure influence acoustic properties. While past research has evaluated the effects of discharge and flow structure on acoustic signals separately in either field or laboratory settings, this study investigates these variables jointly in natural, dam regulated, and laboratory fluvial settings. To elucidate the roles of discharge and flow structure on acoustic signals, this study examined sound from eight stream-gauged, morphologically diverse study sites, a discharge-variable morphologically constant flume plunge-pool, and a morphologically variable discharge-constant plunge-pool. Rising

downstream depth at a plunge-pool strongly influences both acoustic power and frequency. The initial drop height of a plunging jet and the width of its receiving pool were found to clearly influence acoustic signals, while the width of a plunging jet may also play a role in acoustics. Using sound to infer discharge works well at step features with low width/depth ratios, at high width/depth ratio step features with negligibly changing morphologies, and sometimes works at riffle features and morphologically variable step features. At several field sites, we observed power to increase with flow until a certain discharge threshold, where it either does not change or decreases with rising discharge. With additional studies in morphologically diverse channels such as bedrock and cascade, acoustics may be used as a non-invasive, inexpensive, and accurate hydrometric tool to help fill global surface water gauging gaps.

TABLE OF CONTENTS

LIST OF FIGURES

LIST OF ABBREVIATIONS

Fr	Froude Number
W/D	width/depth

CHAPTER ONE: BACKGROUND

1.1. Stream Discharge

This study aims to observe the relationship between sound and stream discharge. Stream discharge is the volumetric rate of flow (volume per unit time) of water flowing through an open channel. The U.S. Geological Survey (USGS) measures stream discharge tens of thousands of times annually using several techniques to meet irrigation and drinking water demands, assess the impacts of climate-change on finite freshwater resources, and monitor potentially hazardous floods (Buchanan et al., 1976). Although discharge cannot be measured directly, it can be inferred from empirical variables such an incoming flow's width, depth, and velocity. The most common and practical method of continuously measuring discharge involves joint use of continuous stage (depth) measurements with calibration using the velocity-area method, where discharge is computed as the product of incoming flow's cross-sectional area and average velocity. This computation can be represented by the equation:

$$Q = \sum_{i=1}^{n} a_i v_i \qquad (1)$$

where Q is the total discharge in ft^3 or m^3/s, a is cross sectional area, in ft^2 or m^2, of the ith section of n sections in which the cross section is divided, and v is the corresponding mean velocity, in ft or m/s, of each vertical ith section (Figure 1.1).

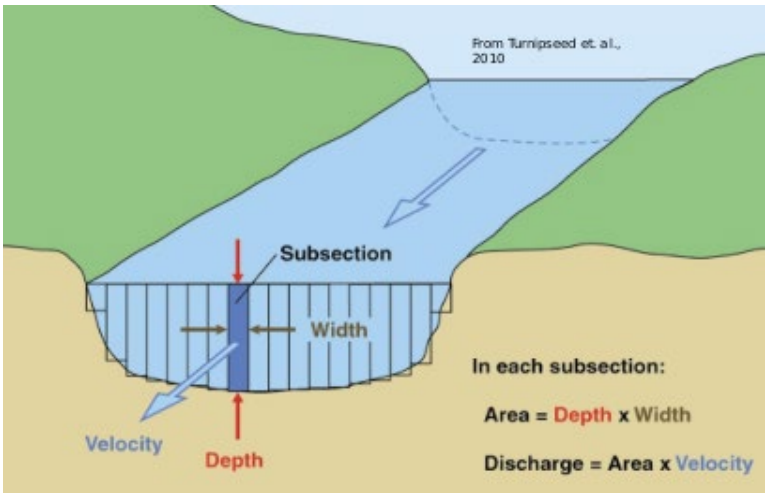

Figure 1.1. A cartoon visualizing the velocity area method of calculating stream discharge.

A flow's width and depth can be measured by a hydrographer wading into a stream channel, using an existing structure such as a bridge of concrete or ice, constructing a cableway which transports a hydrographer across a channel, or by using a boat. To continuously track discharge, an installation of in-stream, depth measuring infrastructure is used and calibrated by discrete velocity-area measurements. The need to develop invasive and expensive infrastructure to continuously measure stream discharge calls for new, innovative methods of stream discharge gauging (Hannah et al., 2011).

1.2. Acoustics

Acoustics is a subset of physics which studies sound, or mechanical disturbances (waves) through an elastic medium (solids, liquids, gases). Earth scientists are typically interested in energetic Earth processes that create sound waves, propagating from a dynamic source to a receiving microphone. In fluid mediums such as air and water, sound waves are deviations from an ambient pressure level. These pressure deviations can be quantified in terms of their wave amplitude and frequency of oscillation (Figure 1.2).

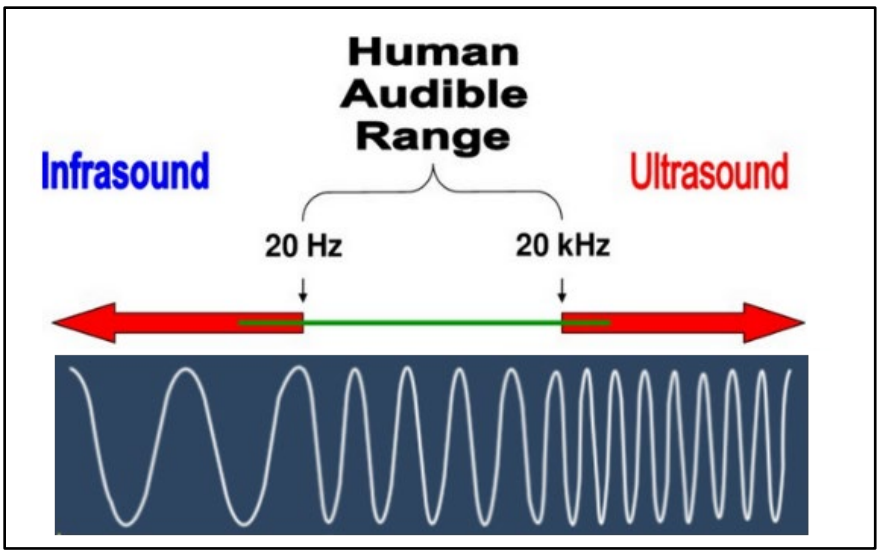

Figure 1.2. The acoustic frequency spectrum, at constant amplitude.

Sound wave amplitude is the magnitude of local deviation in pressure, measured in Pascals. A pascal is the pressure exerted by 1 Newton of force normal to a 1 m^2 area. The square of a sound signal's amplitude is its power, measured in Pa^2. Calculating a signal's power accounts for both negative and positive amplitude variations. The frequency of a sound signal may be intuitively thought of as its pitch, or tune, but is mathematically defined as how many times its sound waves oscillate per second (Hz). Any sound signal can be decomposed into several discrete frequencies, or a spectrum of frequencies, which contain information about its source and propagation. The geometry of an acoustic source and the propagation distance to its receiver will influence the recorded power and frequency signals. Larger sources generally emit lower frequency signals which are slower to attenuate (lose power) due to their long wavelengths, and a greater distance between a source and its receiver results in greater power loss from attenuation. Higher frequencies generally lose power at smaller source-receiver distances and timescales. A spectrogram is a time-domain representation of the frequency spectrum that composes a

sound signal (Figure 1.3). Within a spectrogram, brighter colors opposed to a dark background level indicate a higher concentration of power at that particular frequency. Atmospheric and anthropogenic noises plague the lower end of the sound spectrum from sources such as ocean waves, storms, machinery, and vehicles, creating a need to eliminate (filter) signals at unwanted frequencies in this study.

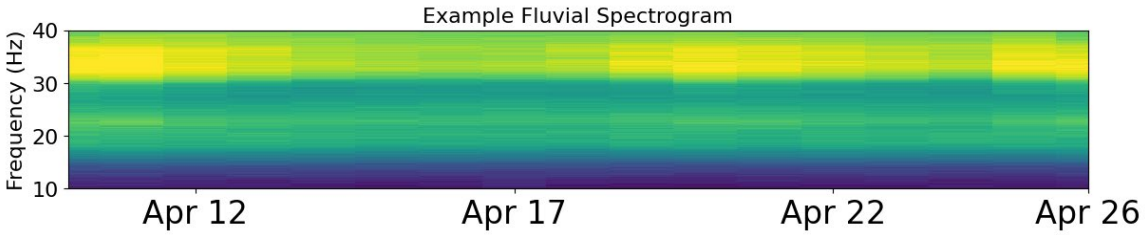

Figure 1.3. An example of a spectrogram from a fluvial signal recorded in April 2021. Brighter yellow colors indicate higher acoustic power at a given frequency, while blue represents no sound power at a particular frequency. In this case, filtering out frequencies below 10 Hz eliminates unwanted environmental noise.

This study's overall goal is to quantify the acoustic response to changing discharge at various stream channel features, therefore it is imperative to understand how common channel morphologies dissipate hydraulic energy and respond to changes in discharge. Stream channel gradient and morphology determine the morphology, frequency, and primary energy dissipation mechanisms of streamflow (for example hydraulic jump or plunging jet; expanded upon in Chapter 2 Introduction) and how their flow structures vary with discharge (Chin et al., 2009). Field campaigns have provided measurements of channel features such as slope, confinement, sediment size, and width/depth (W/D) ratio creating a morphological framework within which to simulate channel responses to inputs such as discharge, sediment supply, and sediment transport

capacity (Montgomery & Buffington., 1997). While natural river features fall into a continuum of these classifications, it is practical to morphologically sort channels and reaches to understand how fluvial sound sources are generated, how they behave at a range of discharges, and how to identify common features of successful acoustic stream gauging sites. Understanding how channel morphology influences discharge-sound relationships at common channel variations can bring acoustics from a promising idea to an established hydrometric tool.

1.3. Channel Morphology

Alluvial stream channel morphologies can be described by five unique reach types: Cascade, step-pool, plane bed, pool riffle, or dune ripple (Montgomery & Buffington, 1997):

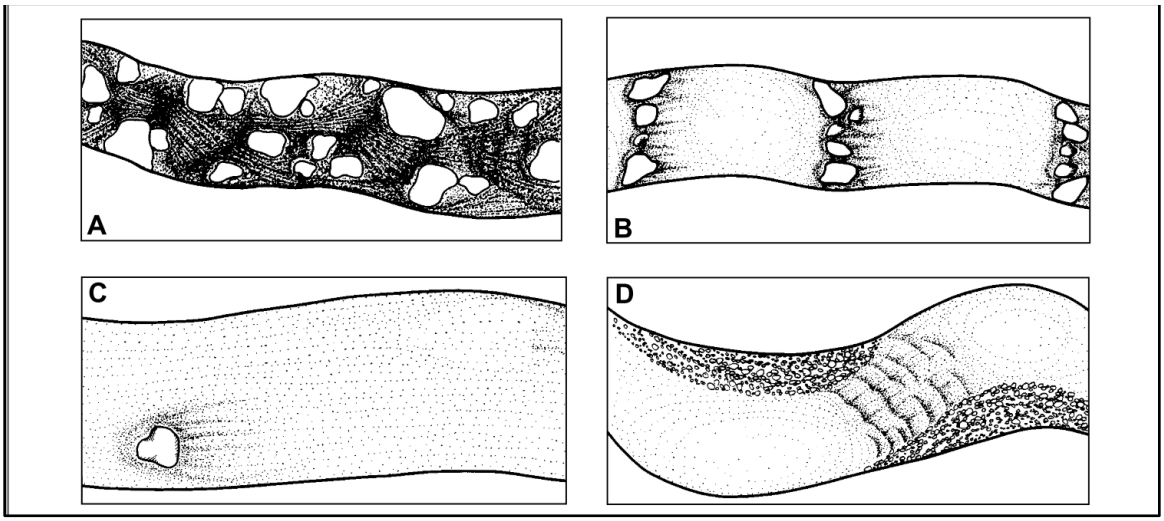

Figure 1.4. An aerial view of four common mountain channel reach morphologies. A: Cascade B: Step-pool C: Plane bed and D: Pool-riffle

High gradient and elevation channels (cascade, step-pool) generally have high ratios of sediment transport capacity to sediment supply and are morphologically stable at a range

of discharges. Low gradient and elevation channels (pool-riffle, dune-ripple) have a high supply of sediment relative to their transport capacity and therefore display significant morphological responses (sediment erosion/deposition) to changes in discharge. A long-term acoustic response to changing discharge is likely dependent on how flow structure varies with discharge. Variables such as channel gradient, watershed elevation, channel morphology, and width/depth ratio may affect the consistency and form of discharge-sound relationships by altering flow structure.

Pool-riffle reaches occur at low gradients, low watershed elevations, and are unconfined with well-established floodplains (Montgomery & Buffington., 1997; Figure 1.4 D). Pool riffles consist of an oscillating, rhythmically spaced bedform with topographic depressions (pools) and alluvial bar rises (riffles). The acoustics of riffle features have not been studied, however the laterally unstable bed and possible alteration of surface flow structure at high stages forecast a complex acoustic response to changing stream discharge.

Step-pool channel reaches contain large clasts which organize into steps where higher elevation and velocity plunging streamflow impinges pools of lower elevation and velocity (Figure 1.4 B). Step pool morphology is associated with high elevations and channel gradients, valley confinement, and small W/D ratios. Large, bed forming clasts are relatively immobile during flooding events, but extreme floods may move grains of all sizes. While pool-riffle bedforms typically oscillate laterally and longitudinally, step-pool bedforms oscillate vertically and streamwise as plunging streamflow scours the channel bed, creating a hole where finer sediment frequently accumulates. As streamflow free falls into pools, an air entraining impact dissipates kinetic energy, forming

whitewater whose morphology depends on the morphology of the incoming flow and its receiving pool (Pagliara et al., 2008). The channel stability and the energy dissipating impact of streamflow in step-pools forecast a dynamic relationship between discharge and sound. A vertically oscillating bed may be a cause of uncertainty between discharge and sound at step-pool reaches, however the presence of large, difficult to mobilize clasts could yield a consistent acoustic response to changing discharge.

Cascade channel reaches are at high watershed elevations, consisting of tumbling flow down steep slopes in narrowly confined valley walls (Figure 1.4 A). Bed materials are laterally and longitudinally disorganized, with large, immobile cobble and boulder sized clasts providing strong resistance to flow. As flow is forced over and around bed forming clasts at high velocities, much of the kinetic energy is dissipated by hydraulic jumps and plunging jets (Chapter 2 Introduction), resulting in a high concentration of whitewater features. If bed forming clasts remain stable and unsubmerged at high discharges, the frequency and morphology of whitewater features may change predictably with discharge. The presence of many large, immobile clasts in a cascade/step-pool reach makes morphological changes at the reach scale less likely, and channel reaches with steady morphologies are hypothesized to be strong acoustic stream gauging sites. In addition, a high concentration of whitewater in a reach may produce loud acoustic signals, ideal for remotely monitoring discharge.

To elucidate the roles of discharge and channel morphology on acoustics at plunge-pool features, I designed two experiments. I present acoustic recordings of a flume plunge-pool with constant morphology and variable discharge. In addition, I designed and built an adjustable plunge-pool apparatus based on scaled field site

dimensions and kept discharge constant while manipulating pool and jet morphology. To understand how channel size and morphology influence discharge-sound relationships in natural fluvial settings, I analyzed continuous, long-term, broadband recordings of sound from eight stream gauged, morphologically unique study sites. For sites with sufficient data, I present acoustic model curves which estimate discharge from a sound recording.

CHAPTER TWO: DEPENDENCE OF SOUND ON DISCHARGE AND MORPHOLOGY

Rivers, streams, and tributaries play a critical role in the global water cycle and their dispersion of freshwater is essential for widespread human consumption, crop irrigation, waste management, and hydropower generation. Currently, there is a need for innovative, non-invasive, and low-cost methods of surface freshwater discharge monitoring. With careful site selection, recording the acoustics produced by streamflow could be used reliably and inexpensively to infer changes in local discharge. An important knowledge gap currently preventing the use of acoustic gauging is the unknown relationships by which stream sounds depend on discharge and stream morphology. To address this, I record and characterize sound and infrasound produced by morphologically unique features of the Boise River and Dry Creek in Southern Idaho across multi-year spans. Using a flume and a custom-made adjustable plunge-pool apparatus, I record acoustics produced by plunge-pool flow conditions at several scales of discharge and morphology to understand how channel and flow structures influence acoustic properties. While past research has evaluated the effects of discharge and flow morphology on acoustic signals separately in either field or laboratory settings, this study investigates these variables jointly in natural, dam regulated, and laboratory fluvial settings. To elucidate the roles of discharge and flow morphology on acoustic signals, this study examined sound from eight stream-gauged, morphologically diverse study sites, a discharge-variable morphologically constant flume plunge-pool, and a

morphologically variable discharge-constant plunge-pool. Rising downstream depth at a plunge-pool strongly influences both acoustic power and frequency. The initial drop height of a plunging jet and the width of its receiving pool were found to clearly influence acoustic signals, while the width of a plunging jet may also play a role in acoustics. Using sound to infer discharge works well at step features with low width/depth ratios, at high width/depth ratio step features with negligibly changing morphologies, and sometimes works at riffle features and morphologically variable step features. At several field sites, I observed power to increase with flow until a certain discharge threshold, where it either does not change or decreases with rising discharge. With more studies in morphologically diverse channels such as bedrock and cascade, acoustics may be used as a non-invasive, inexpensive, and accurate hydrometric tool to help fill global surface water monitoring gaps.

2.1. Introduction

There is a large data gap in surface freshwater hydrology that must be filled with innovative solutions. Stream gauges in the U.S. primarily monitor high-order streams while low order streams are severely under-monitored and their roles in a watershed are relatively unknown (Hannah et al., 2011). Global stream gauge resolution is overrepresented (though still coarse) in the global north and underrepresented in the global south. This gauge coverage insufficiently represents the overall variability of Earth's fluvial systems, and surface hydrologists are calling for greater investment in stream gauging infrastructure (Krabbenhoft et al., 2022; Hannah et al., 2011). An improved understanding of large-scale hydrologic processes, using stream gauging

techniques, is necessary to sustain socio-economic growth and provide global water, food, and energy security (Hannah et al., 2011).

Widely used stream discharge gauging methods require constant measurement of stage as a surrogate variable to infer discharge through an empirically derived stage-discharge relationship (Chow, 2007; Buchanan et al., 1976). To ensure USGS stream gauging accuracy standards, a hydrographer may also need to measure a flow's cross-sectional area and velocity field multiple times per year (Buchanan et al., 1976). The processes and instrumentation used to continuously monitor river stage are invasive to the river's channel, may be damage-prone or difficult in flooding conditions, and may be expensive to annually maintain (Buchanan et al., 1976). For these reasons, there is a critical global need for accurate, cost-effective, and non-invasive methods of surface freshwater discharge monitoring (Chacon-Hurtado et al., 2017).

2.1.1. Physics & Acoustics of Streamflow

The recording of passive acoustics, including both infrasound (frequencies <20 Hz) and audible sound (20-20,000 Hz frequencies), has been utilized as an inexpensive, resilient, and remote monitoring tool for surface flow processes (Park et al., 2008; Lyons et al., 2021; Odzer & Francke, 2020). Streamflow produces sound at a wide range of frequencies and through various mechanisms (Osborne et al., 2021; Schmandt et al., 2013; Ronan et al., 2017; Podolskiy et al., 2023; Tatum et al., in press).

A hydraulic jump is a previously studied fluvial acoustic source where a shallow upstream flow abruptly slows and deepens downstream (Chow, 2007; Ronan et al.,

2017). Hydraulic jumps are classified using the dimensionless Froude number (Fr) (Chow, 2007):

$$Fr = \frac{v}{\sqrt{gd}} \quad (2)$$

where v is the depth averaged velocity, d is the local depth, and g is the acceleration due to gravity. A hydraulic jump dissipates energy as flow transitions from supercritical (Fr>1) to subcritical (Fr<1). The kinetic energy dissipation of a hydraulic jump, characterized by a foamy whitewater appearance and air entrainment, releases heat and generates measurable seismoacoustic signals which partially depend on the jump morphology (Ronan et al., 2017). In open channels, the Fr may be an incomplete descriptor of whole-reach characteristics, however it is a useful hydraulic classifier of open-channel streamflow.

A liquid plunging jet or plunge-pool is a free falling, cohesive column or plane of liquid impinging a horizontal pool of the same liquid. The plunge-pool is a commonly found, consistent, and loud fluvial acoustic mechanism due to a point-source impact which shears entrained air pockets into bubble plumes and vortices (Evans et al., 1996). The flow structure of whitewater produced by a plunge-pool depends on several parameters, including air entrainment, jet geometry and impact velocity, tailwater pool depth, and tailwater pool morphology (Pagliara et al., 2008). Few studies have measured the acoustics (measured underwater and above water) at plunge-pools with variable morphologies to estimate bubble plume size distributions (Boyd & Varley, 2003; Odzer & Francke, 2020; Chanson & Manasseh, 2003), and plunging ocean waves to elucidate

the source of infrasound (Park et al., 2008), but the effects of discharge on acoustics at plunge-pools are not well understood.

Past work shows that fluvial acoustic signals depend on both discharge and a whitewater feature's morphology. Schmandt et al., (2013) first recorded seismoacoustic signals at a controlled flood in the Grand Canyon, attributing infrasound (< 20 Hz) to waves breaking at the water surface. This study showcased the potential use of acoustic power for monitoring discharge in hazardous flood conditions, but only recorded a single reach. Ronan et al., (2017) found a relationship between infrasound power and Froude number at an adjustable whitewater wave, namely that a Froude number of 1.7, corresponding to a discrete change in hydraulic jump morphology, must be exceeded to generate coherent infrasound signals. The finding of an inverse correlation between Froude number and the power of the dominant acoustic frequency agreed with previous empirical studies (Mossa, 1999; Chachereau & Chanson, 2011). Ronan's study first explored the influence of discharge and flow morphology on acoustics but lacked spectral measurements above 40 Hz commonly produced by rivers, and only observed a single site. Osborne et al. (2021) attributed changes in the audible sound (>50 Hz in this study) and stage relationship to the submergence of in-channel roughness elements when stage increases from low to high levels. In addition, the authors qualitatively correlated sound pressure level to the presence or absence of whitewater in a channel reach. This study showed promising relationships between sound and stage at multiple sites, calling for longer-duration studies in morphologically diverse stream settings. Podolskiy et al. (2023) showed positive correlation between acoustic power and glacial discharge across a month-long campaign but lacked site morphological diversity and long-duration

observations. The authors observed hysteretic behavior; steeper rises in sound power compared to rises in discharge, and less steep falls in sound power compared to falls in discharge. This and other previous work suggest that the discharge-sound relationship may be inconsistent due to discharge dependent flow structures in stream channels, which also cause uncertainties in stage-based gauging. In addition to the above research studying fluvial acoustics, inferring sediment transport rate from seismoacoustic signals has been an interest to fluvial geomorphologists, hydrologists, and civil engineers. Seismic fluvial studies have been used to refine theory based numerical models which predict sediment transport (Gimbert et al., 2014; Tsai et al., 2012; Hsu et al., 2011). Hydroacoustics, which measure underwater sediment generated noise, have determined bedload transport rates, grain size distributions, and quantified bed topography effectively in field settings (Mao et al., 2016, Marineau et al., 2019, Petrut et al., 2018, Le Guern et al., 2020). Although interesting, sediment transport is not in the present study's scope and at our study sites we consider it to be an insignificant source of sound (changes in bed morphology could explain hysteretic acoustic trends, however).

To understand how channel size and local flow structure influence discharge-sound relationships in natural fluvial settings, we analyze continuous, long-term, broadband recordings of sound from eight gauged study sites of various scale with diverse flow structures. For sites with sufficient data, we present acoustic model curves which estimate discharge from a recording of sound. To further elucidate the roles of discharge and channel morphology on acoustics at plunge-pool features, we measure sound in two experiments. We first present recordings of a flume plunge-pool with constant morphology and adjustable discharge. Next, we design and build an adjustable plunge-

pool apparatus based on scaled field site dimensions with constant discharge and adjustable pool and jet dimensions. Revealing the roles of discharge and morphology on acoustics at several fluvial scales can help bring acoustic stream gauging from a promising idea to a useful hydrometric tool.

2.2. Methods

Our primary study sites, the Boise River and Dry Creek, lie in dynamic alluvial mountain stream channels in Southwest Idaho that are frequently influenced by anthropogenic and natural disturbances (Montgomery & Buffington, 1997). The Boise River is an anthropogenically confined, dam regulated, pool-riffle stream channel with a high width/depth (W/D) ratio (Richardson & Guilinger, 2015). Within the Boise River, we recorded acoustics from three discrete, flow diverting step/drop features and two low-slope riffle features. The Dry Creek Experimental Watershed (DCEW) contains several valley-confined, natural channels with small W/D ratios. Within DCEW, we recorded acoustics from three step-like features: one with a discrete plunge-pool and two with spilling/tumbling flow. To elucidate the controls on acoustics at cohesive plunging jets over a discrete, step-like feature, I recorded a flume and a custom made, adjustable plunge-pool apparatus to simulate several fluvial scenarios. I first describe methods of collecting and processing field data, followed by the construction and manipulation of the plunge-pool apparatus, and finally the Streamlab flume recording procedures.

2.2.1 Field Methods

In the field, Gem infrasound loggers (Anderson et al., 2018) and AudioMoth audible-sound loggers (Hill et al., 2019) were installed out of the channel and hidden in riparian vegetation for a time-span dependent on power supply. With sufficient power supply and storage capacity, battery changes and data retrieval were required once every 2-4 weeks. Microphones were placed <30 meters from larger and more energetic, lower frequency emitting features, and <5 meters from smaller, less energetic, higher frequency emitting features. When selecting a site, we first ensured that the reach was audibly loud (Osborne et al., 2020), that sensors could be safely concealed out of direct sight (Anderson et al, 2018), and that sensors would not be impacted by flooding of the channel or significant rainfall accumulation. Gem infrasound loggers reliably record frequencies from 1-40 Hz and can record up to 115 Pa without clipping (a very high amplitude that is unlikely to be produced by rivers). The instrument is installed within a weather-proof enclosure that is small, lightweight, and easily installable in the field. One Gem costs only a few hundred dollars, two orders of magnitude less than a typical USGS stream gauge. We programmed audible sound sensing (50-8000 Hz) Audiomoths to conserve power by turning on and recording for 30 seconds on the hour. Audiomoths are credit-card sized (58 x 48 x 18 mm) and low cost (around 100 USD), making them ideal for long-term, large scale scientific studies in challenging terrains (Hill et al., 2018). Both sensors output data to microSD cards, and their combined use ensures a signal bandwidth between 1 Hz and 8 kHz (Anderson et al., 2018; Hill et al., 2018). This frequency range fully encompasses the acoustics produced by fluvial features in this study and past fluvial acoustic studies (Ronan et al., 2017; Osborne et al., 2020; Podolskiy et al., 2023). The

size of the fluvial acoustic source dictated which sensor was used at a site, as smaller sources with lower discharge were not found to produce infrasound.

With signal processing and data selection, constant river signals were extractable from potentially complex soundscapes. When working with long-term acoustic field data, we selected an hour with less wind and anthropogenic noise (03:00-04:00 local time) to represent a day and applied a site-dependent Butterworth, 4 pole, digital high-pass filter above 1 Hz to preserve river signals and eliminate common noise at low frequencies. Once filtered, Welch's method was used to calculate the average power spectrum over time, which further ensured that the signal was not affected by transient noise. Upon calculation of the acoustic spectra, we computed the integral of the average power spectrum and calculated the overall spectrum's mean frequency. We use mean frequency as a stable estimate of the signal's dominant frequencies; a simpler alternative measure, the peak frequency, is less useful due to its high sensitivity to minor changes in spectra. Both power and mean frequency were used as metrics to track how sound varies with discharge. The Boise River discharge records were extracted directly from the USGS gauge #13206000 located downstream of the study sites (USGS, 2021). DCEW discharge records came from Boise State University's Department of Geosciences stage-discharge rating curves (McNamara, 2017). We acknowledge potential uncertainties in discharge measurements at both channels from common problems such as sediment and debris accumulation, channel erosion, instrument malfunction, and data quality control error. For the Boise River, small tributaries, diversions, and returns are other possible sources of error in local discharge. Once fluvial acoustic signals were properly conditioned, we plotted sound power and mean frequency as a function of discharge to produce acoustic

model curves. Power and mean frequency were calculated in either the entire 5-40 Hz band for Gem data, or the 50-8000 Hz band for Audiomoth data. For sites with sufficient data, we used polynomial curve fitting methods to produce models which describe the long-term trend of the data. The form of the acoustic model curves were compared by feature morphology (jet or riffle) and channel size (W/D ratio).

The unique form of acoustic model curves at plunge-pool sites warranted the study of plunge-pool acoustics in controlled settings. Thus, we designed two additional experiments to quantify the acoustic response to changing discharge and channel morphology at plunge-pool features.

2.2.2 Flume Experiment Methods

To simulate rising discharge at an unchanging channel morphology, we recorded acoustics from a plunge-pool flume. The University of Idaho's Streamlab Flume consists of a 20 meter long, 2 meter wide, and 1.2 meter deep channel (Figure 1). Its flow, with a maximum discharge of 1.1 m^3/s, plunges from a height of 2 meters into a 4 meter deep pool with a surface area of over 60 square meters. The pool and channel are contained entirely by concrete and glass (Figure 1).

Figure 2.1. A front view [A], side view [B], and main channel view [C] of the Streamlab Flume plunge-pool.

Using a Chaparral infrasound microphone (Slad et al., 2016), a DATACUBE data logger, and several Audiomoths, we sampled the acoustics at eight recorded discharges, provided by the flume's built in flow meter. Upon each iteration, we allowed discharge to stabilize before powering on Audiomoths to record while the Chaparral infrasound microphone recorded continuously, consistent with our field methods. With this data, we plotted both audible and infrasound power and mean frequency at each recorded iteration and filtered out low frequency (<5 Hz) noise from the flume's pump.

2.2.3 Adjustable Plunge-Pool Methods

To explore the dependence of sound on morphologies of plunging jets, tailwater pools, and interfacial flow structure at plunge-pools, we assembled an adjustable plunge-pool apparatus using a submersible hydraulic pump, garden pavers, plexiglass, 2 kiddie pools, and a water storage reservoir (Figure 2). The submerged pump routed water from the pump's water storage pool (downstream) to the plunging jet's storage reservoir (upstream) until the reservoir's water level reached the height of the opening. Then, a jet of water plunged into and filled a plexiglass covered, slightly elevated, adjustable bed within a pool where we constrained pool width using garden pavers (Figure 2). In this experiment, we measured sound as a function of filling tailwater pool depth and tracked this relationship across constant jet discharge and variable jet height (measured from the pool base), jet width, and pool width. We used a Nikon D3100 digital camera and an in-pool gauge (ruler) to measure tailwater depth and make visual observations of interfacial flow structure in the pool (Figure 2). To adjust jet width, we first used a jigsaw to create a large flow outlet within the upstream storage reservoir, then applied duct-tape to force flow through outlets of various widths. We used garden pavers to raise a pedestal-like setup on which the storage reservoir rested, increasing the initial jet height. The pool width was adjusted by widening or narrowing side-resting garden pavers, which were placed on a paver supported, plexiglass channel bed (Figure 2). For all physical model runs, pool depth ranges from 0 to ~15 cm. Jet height above the bottom of the pool was increased in 6 cm increments from 28-40 cm, with default pool widths and jet widths of 80 and 17 cm respectively. Jet width was increased at irregular intervals, from 12-33 cm, with default pool widths and jet heights of 80 and 28 cm respectively. Pool width was

doubled from 20 to 40 cm, and from 40 to 80 cm with default jet heights and jet widths of 40 and 17 cm respectively.

To establish an effective physical model, we measured and scaled down morphological dimensions from Diversion Dam, a large step dam on the Boise River, by a factor of 60. To ensure proper scaling, we maintained Fr similitude between the prototype and model by measuring jet width upstream of the dam, pool width downstream, jet height from the water surface upstream to downstream, and discharge from a USGS stream gauge. Our scaled physical model emulated these measurements (Figure 2). However, we acknowledge that achieving precise similarity among plunging jet flows is challenging due to complex interactions between entrained bubbles and a developing mixing layer (Chanson & Manasseh, 2003).

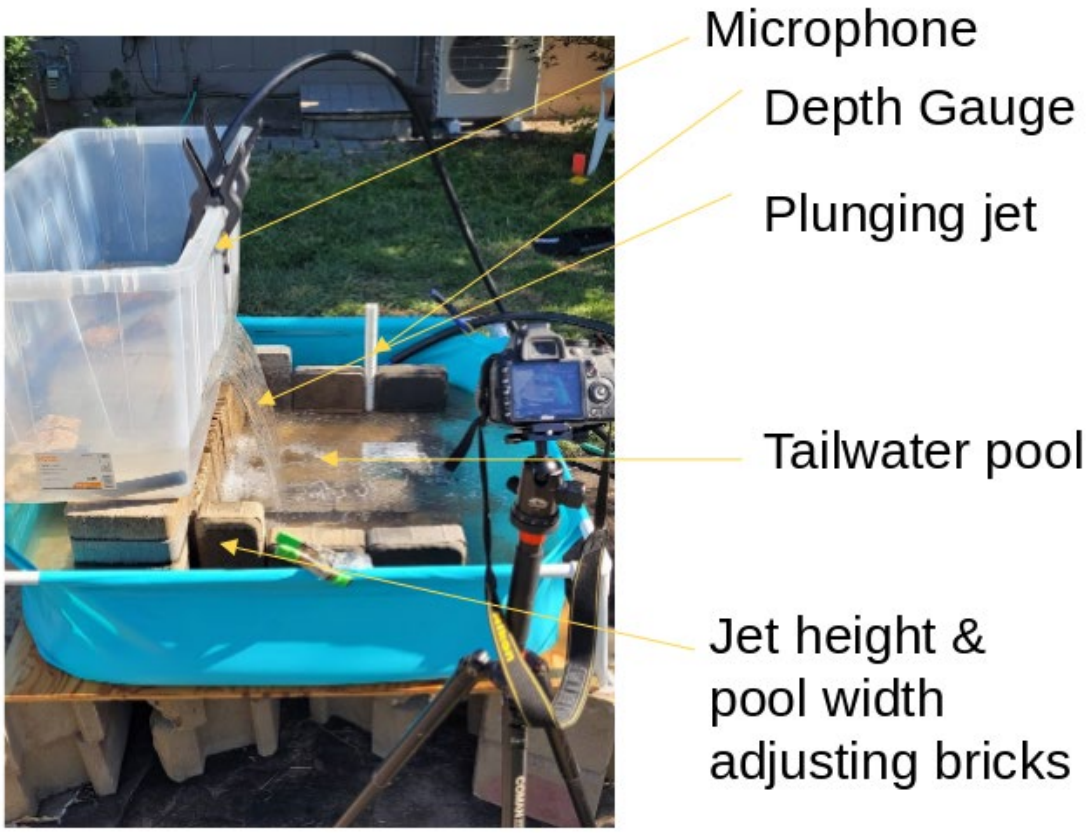

Figure 2.2. Plunge-pool photo demonstrating the experimental setup.

The manipulation of key dimensions jet width, jet height, pool width, and pool depth modeled three possible channel morphological scenarios. In the first scenario, rising tailwater depth changes the magnitude of scour on an alluvial channel bed. As the tailwater rises, the free jet length decreases, changing the energy dissipation and flow structure (Pagliara et al. 2008). In the second scenario, eroding or collapsing channel banks create a jet or tailwater pool with greater width, resulting in less physically constrained flow and a change in energy dissipation. In the third scenario, accumulated sediment in a pool is transported, decreasing the tailwater pool depth and increasing the free jet height. We quantified the acoustic response to changing channel morphological

conditions and observed the depth and morphology dependence on flow structure at a plunge-pool model.

2.3. Results

This study compares discharge, power, and mean frequency data from a flume and eight field sites. For field data, we produce acoustic model curves, which are lines of fit through values of discharge and power or mean frequency calculated from filtered sound pressure values at discrete changes in discharge. Acoustic model curves are differentiated by channel W/D ratio and feature morphology (riffle vs. step). Acoustic information may also be visualized as an acoustic hydrograph displaying time-series A.) Gauged discharge, B.) Power, and C.) Frequency (spectrogram). In addition, this study quantifies the power and mean frequency responses to rising tailwater depth and changing jet/pool morphologies at an adjustable plunge-pool apparatus.

2.3.1. Flume Results: Adjustable Discharge, Fixed Morphology

Figure 3 introduces an acoustic hydrograph, showing power and frequency responses to eight recorded discharges. For the flume experiment, discharge ranges from 0.1-0.8 m^3/s, and the frequency spectrum ranges from 5-8000 Hz by using two instruments: A Chaparal Infrasound microphone sampling at 200 Hz, and an Audiomoth audible microphone sampling at 16 kHz.

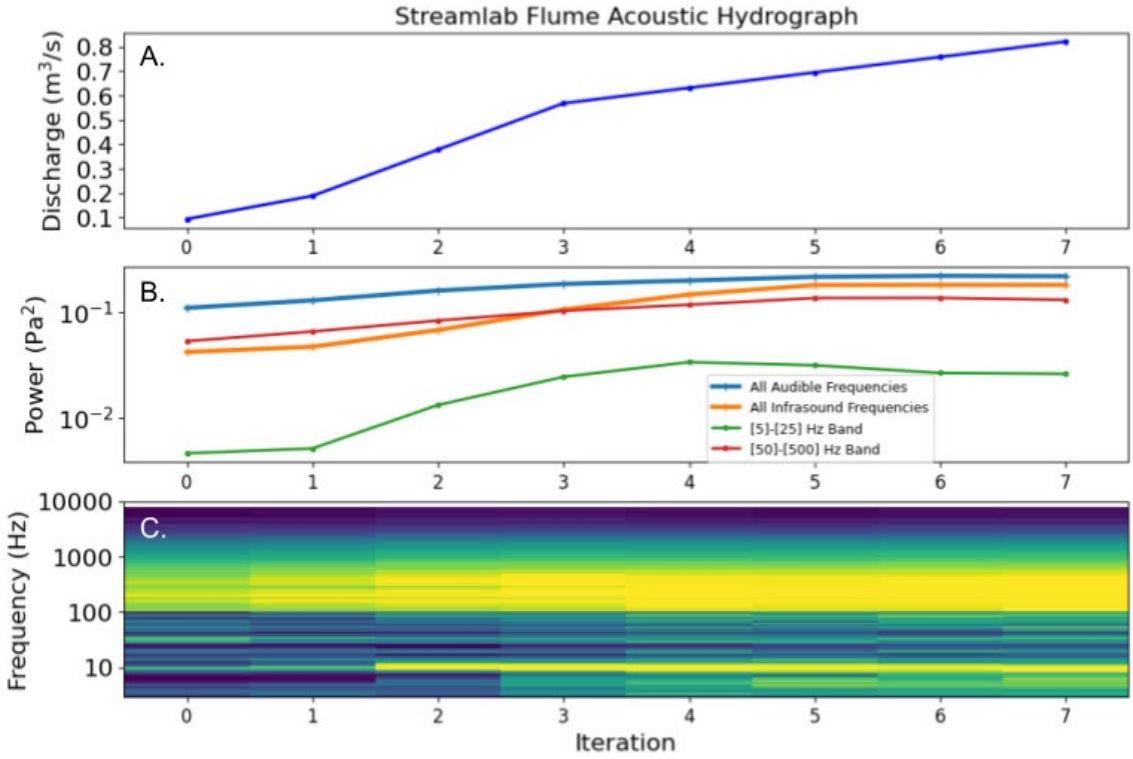

Figure 2.3. Discharge (A), Power in the full audible, full infrasound, lower audible, and lower infrasound bands (B), and audible and infrasound frequency (C) data from the Streamlab flume. Infrasound data recorded by Chaparral ranges 5-100 Hz, and audible data recorded by Audiomoth ranges 100-8000 Hz.

Calculations of power in different frequency bands (Figure 3 B) yield slightly different results, but in all bands power reaches a threshold at 0.694 m^3/s (iteration 5) where it will slightly increase or will decrease with increasing discharge. Bands of 5-25 Hz and 50-500 Hz were chosen because they contained much of the signal's power. Before iteration 5, audible and infrasound power increase when discharge does, but do so at different magnitudes. Mean frequency continuously oscillates for infrasound data and decreases until slightly increasing once reaching iteration 5 for audible data (Figure 4 B).

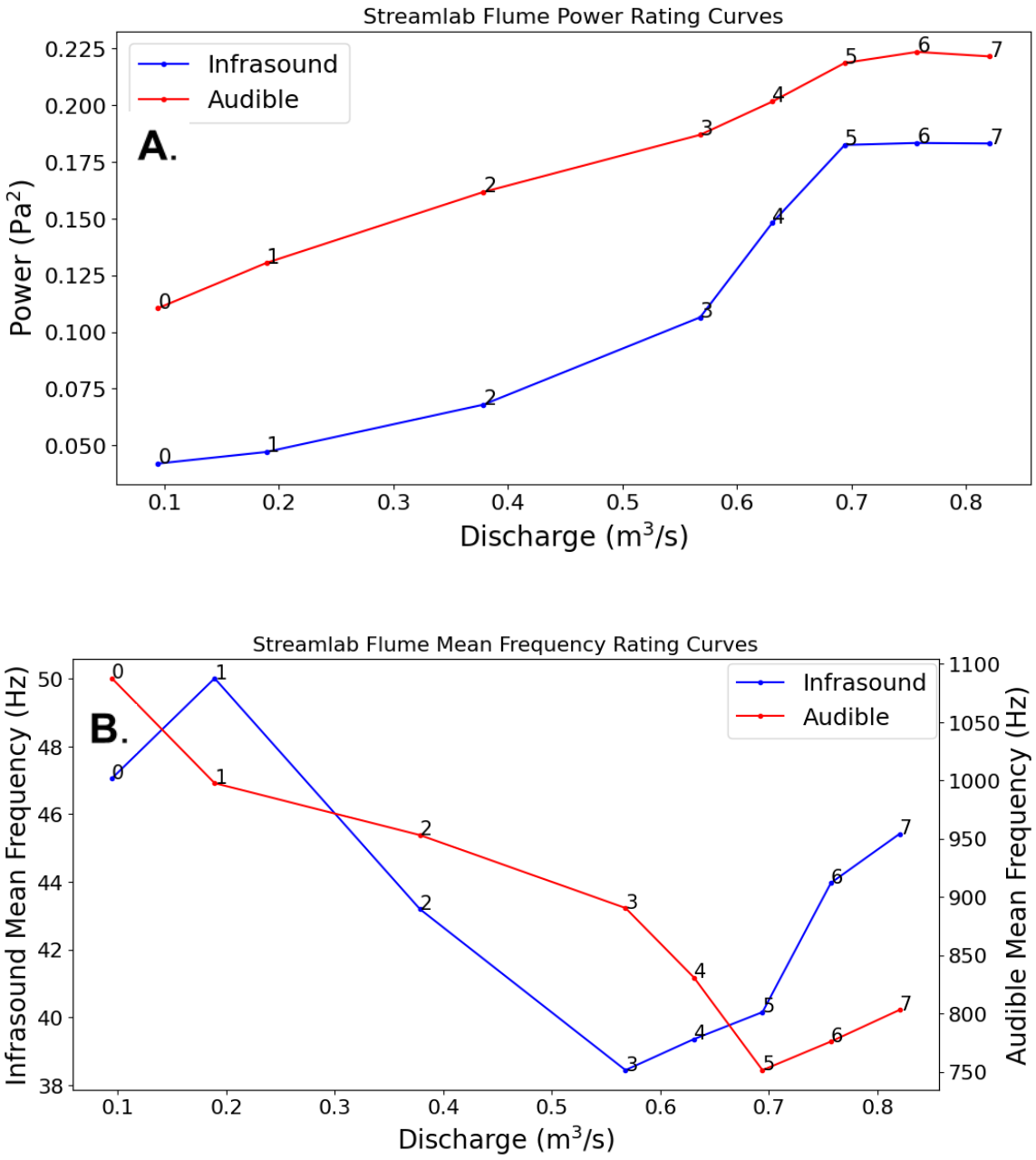

Figure 2.4. Audible and infrasound power as a function of discharge [A], and audible and infrasound mean frequency as a function of discharge [B].

2.3.2. Field Results: Small and Large Channel Responses to Variable Discharge

We present acoustic model curves for data from two Boise River riffle features, three Boise River step features, and three DCEW step features to compare the acoustic responses to changing discharge at large and small W/D ratios and at two variations of flow morphology. Acoustic model curves are generated from a compilation of all available data during the 2021 and 2022 data collection seasons. For Boise River riffles, discharge ranges from < 10 to 80 m^3/s from February to June of 2022. For Boise River steps, discharge is in the same range, but included data is from March 2021 to October 2022. Discharge varies among DCEW step sites, reaching as low as < 0.005 m^3/s for the smallest recorded feature (CON1W) and > 0.45 m^3/s for the largest feature (LG). Data used to calculate DCEW rating curves begins in April 2021 and ends in August 2022. Although data coverage varies by site, Figures 5, 6, and 7 display model curves for Boise River riffles, Boise River steps, and DCEW steps respectively, to compare both power and mean frequency responses over a vast range of discharges.

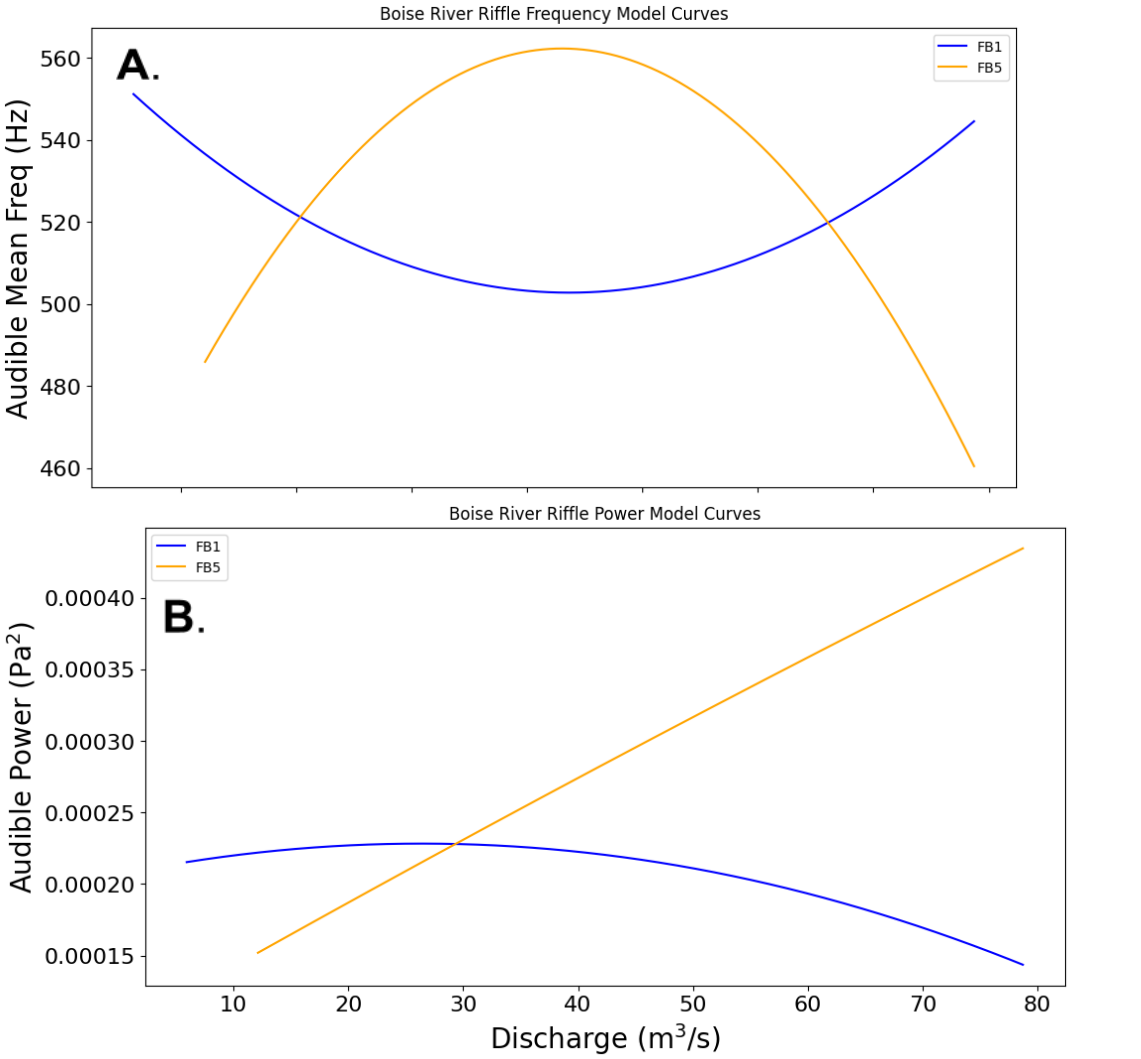
Boise River Riffle Frequency Model Curves
A.
FB1
FB5
Audible Mean Freq (Hz)
560
540
520
500
480
460
Boise River Riffle Power Model Curves
B.
FB1
FB5
Audible Power (Pa^2)
0.00040
0.00035
0.00030
0.00025
0.00020
0.00015
10
20
30
40
50
60
70
80
Discharge (m^3/s)

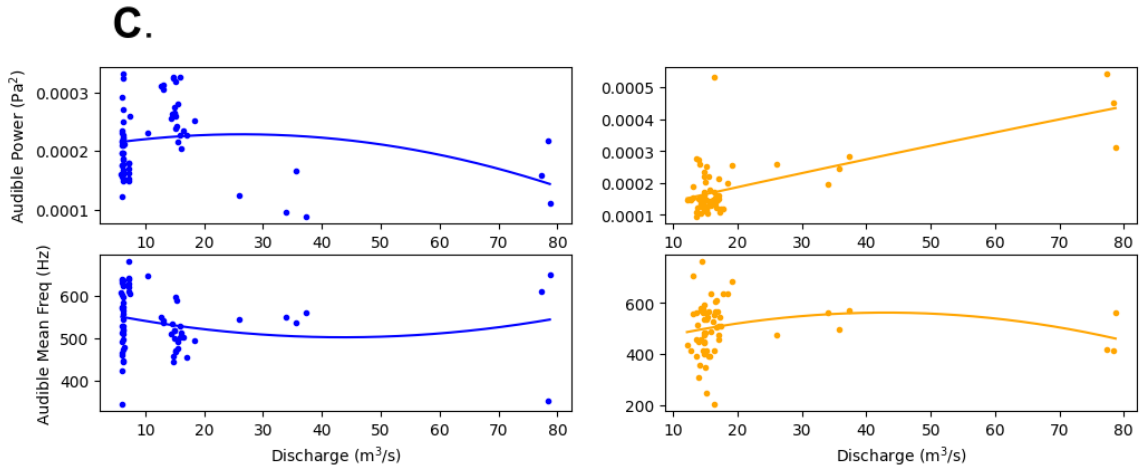
C.
Audible Power (Pa^2)
Audible Mean Freq (Hz)
Discharge (m^3/s)
Discharge (m^3/s)

Figure 2.5. Audible power models [A], mean frequency models [B], and data [C] for two Boise River riffle features as a function of discharge.

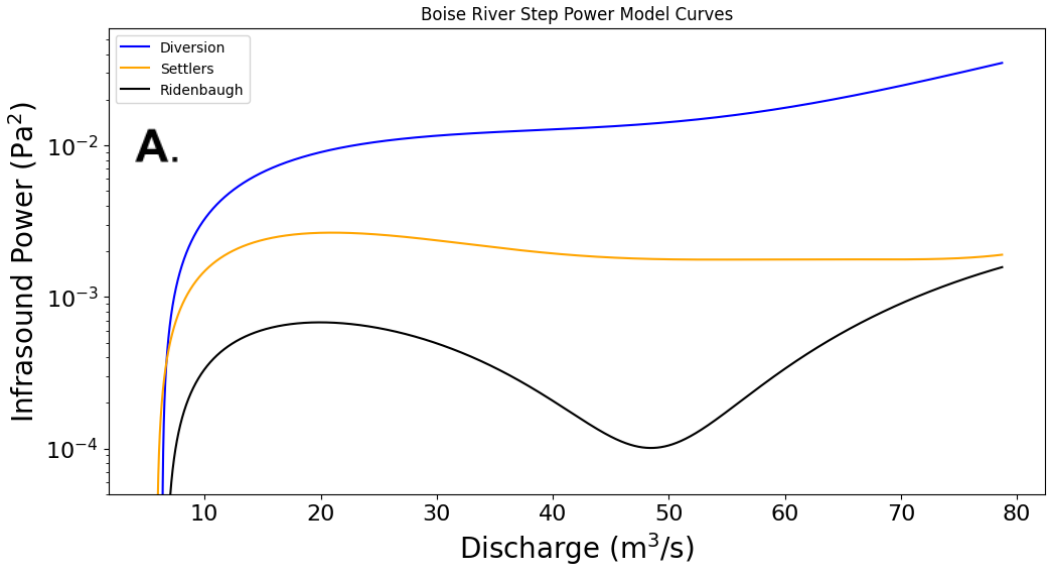
Boise River Step Power Model Curves
Diversion
Settlers
Ridenbaugh
A.
Infrasound Power (Pa^2)
10^{-2}
10^{-3}
10^{-4}
10
20
30
40
50
60
70
80
Discharge (m^3/s)

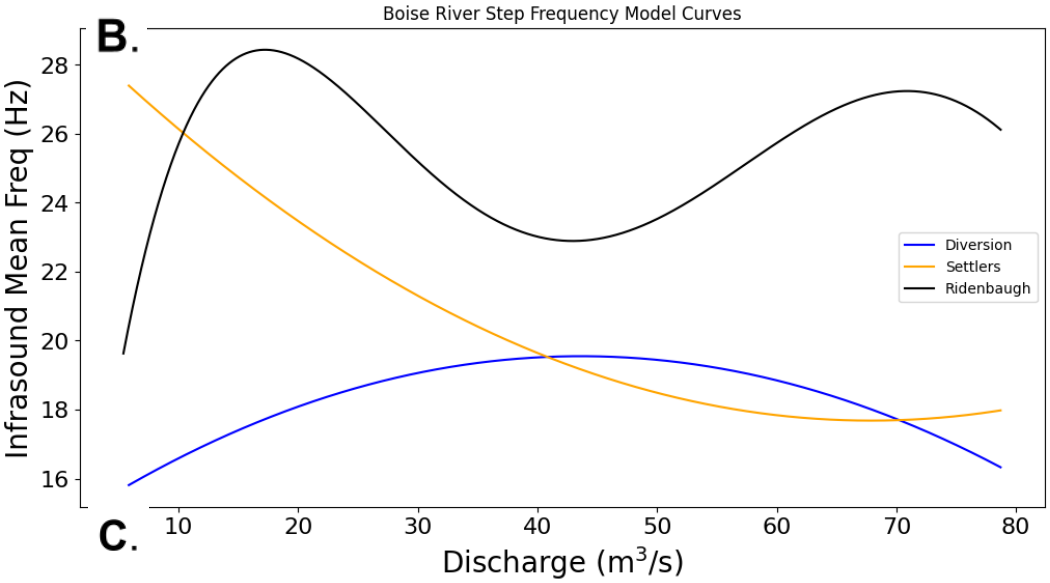
Boise River Step Frequency Model Curves
B.
Infrasound Mean Freq (Hz)
28
26
24
22
20
18
16
Diversion
Settlers
Ridenbaugh
10
20
30
40
50
60
70
80
Discharge (m^3/s)

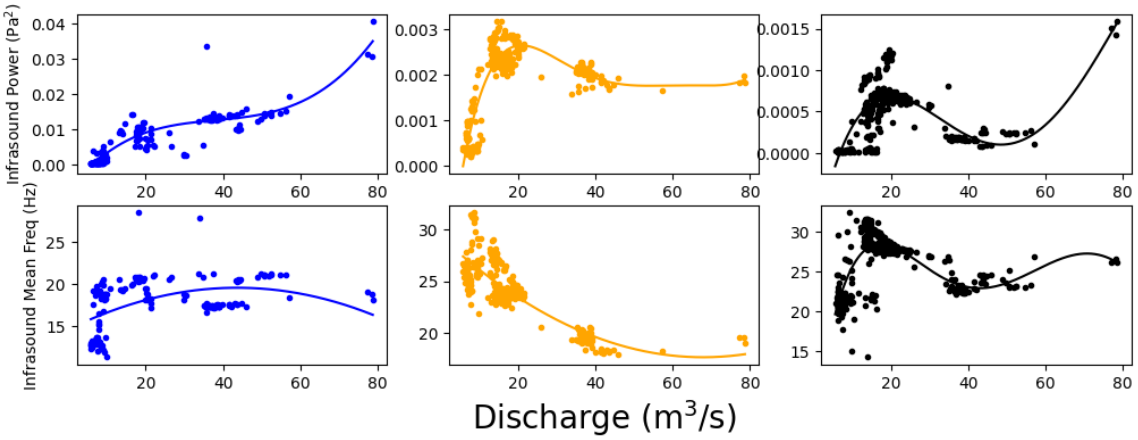
C.
Infrasound Power (Pa^2)
Infrasound Mean Freq (Hz)
Discharge (m^3/s)

Figure 2.6. Infrasound power models [A], mean frequency models [B], and data [C] for three Boise River step features as a function of discharge.

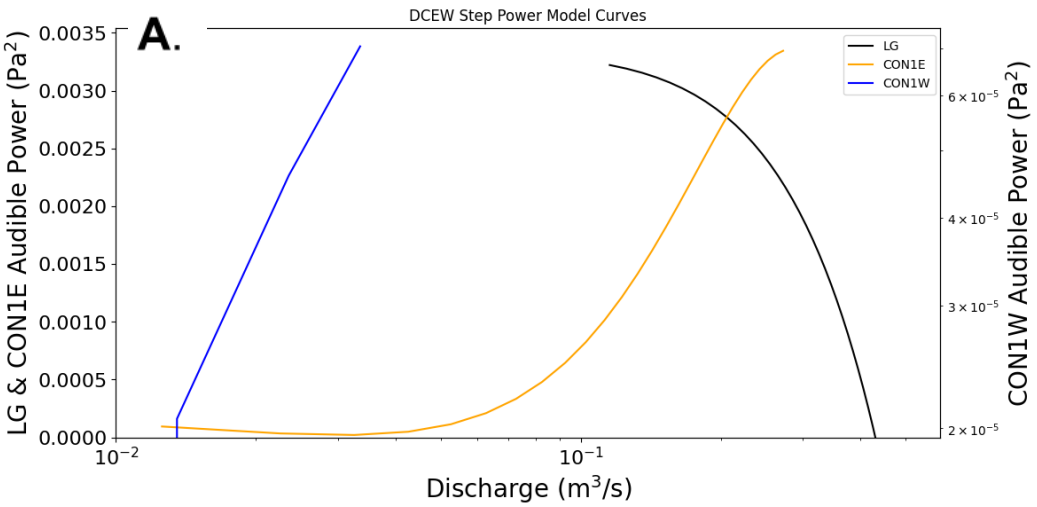

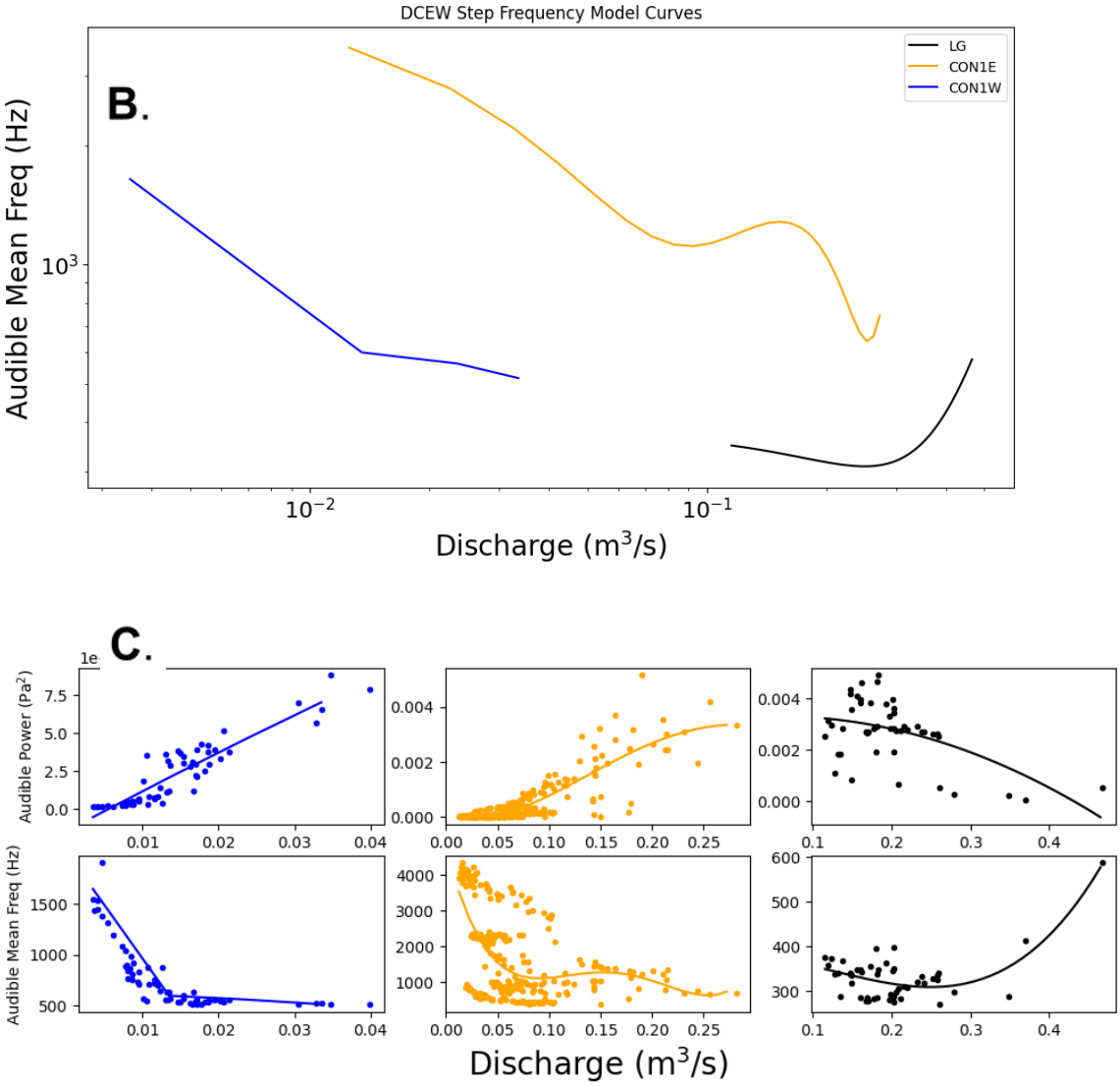

Figure 2.7. Audible power models [A], mean frequency models [B] and data [C] for three DCEW step features as a function of discharge.

At Boise River FB1 riffle, we observe a negative correlation between audible power and discharge, while at Boise River FB5 riffle we observe a positive correlation (Figure 5). FB1's mean frequency decreases until reaching 45 m^3/s then increases back nearly to its original frequency. FB5's behavior is the opposite.

At Boise River Diversion step, infrasound power sharply increases initially, then slowly increases as discharge reaches 80 m^3/s (Figure 6). Settlers power mimics that of

Diversion at first, then begins to slowly decrease until stabilizing around 50 m^3/s. Ridenbaugh power mimics that of Diversion and Settlers, then strongly decreases until 50 m^3/s, where it increases again. The power is greatest at Diversion, due to its high step height, less at Settlers with a lower step height, and least at Ridenbaugh with the lowest step height. Diversion's infrasound mean frequency slowly increases with discharge until 40-50 m^3/s, then slowly decreases as discharge continues to rise (Figure 6 B). Settlers's mean frequency gradually decreases with increasing discharge until reaching 65 m^3/s, where it increases as discharge rises. Ridenbaugh's mean frequency sharply increases with discharge until 20 m^3/s, then sharply decreases until reaching 45 m^3/s, where it increases until 70 m^3/s, then decreases once again as discharge rises. Diversion's mean frequency stays relatively stable, spanning only the 16-20 Hz range, Settlers shows the greatest frequency range of 18-28 Hz, and Ridenbaugh's frequency varies from 20-29 Hz.

Audible power at CON1W increases continuously across the full discharge range (Figure 7). At CON1E, power increases slowly until discharge reaches 0.04 m^3/s, then sharply increases over the remaining discharge range. In contrast, LG's power slowly decreases until reaching 0.2 m^3/s, then sharply decreases. CON1W and CON1E overlap in discharge from 0.015 to 0.03 m^3/s, yet minimum recorded power in this range is an order of magnitude lower at CON1E. Audible mean frequency generally decreases with discharge for CON1E and CON1W but increases at LG (Figure 7 B).

2.3.3. Plunge-Pool Results: Fixed Discharge and Adjustable Morphology

We present recordings of audible power and mean frequency as a function of tailwater pool depth while adjusting three plunge-pool variables: jet height, jet width, and tailwater pool width.

For all recordings, a clear dependence on pool depth was observed for both power and mean frequency (Figure 8). Power rises quickly at first, peaks at shallow pool depths, then falls gradually as whitewater submerges beneath the surface. Upon submergence, power stabilizes and begins to oscillate for the remainder of each recording. Mean frequency oscillates initially, before rising and stabilizing.

A.

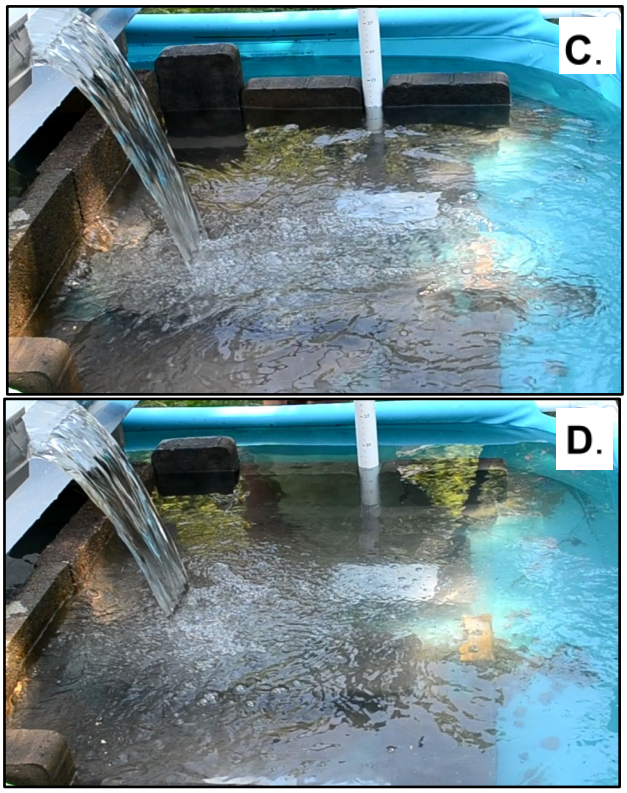

Figure 2.8. An example of variable whitewater morphology as tailwater pool depth increases for the jet height experiment (Jet height = 40 cm). [A] Pool depth = 2 cm, [B] Pool depth = 5 cm, [C] Pool depth = 10 cm, and [D] Pool depth = 15 cm.

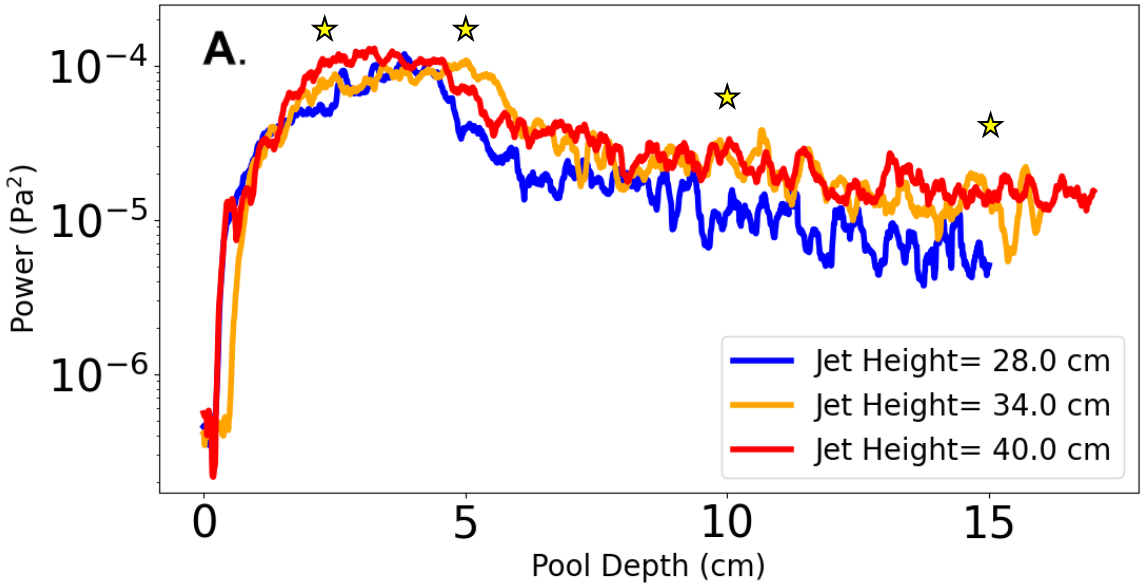
A.
10^{-4}
10^{-5}
10^{-6}
Power (Pa^2)
0
5
10
15
Pool Depth (cm)
Jet Height= 28.0 cm
Jet Height= 34.0 cm
Jet Height= 40.0 cm

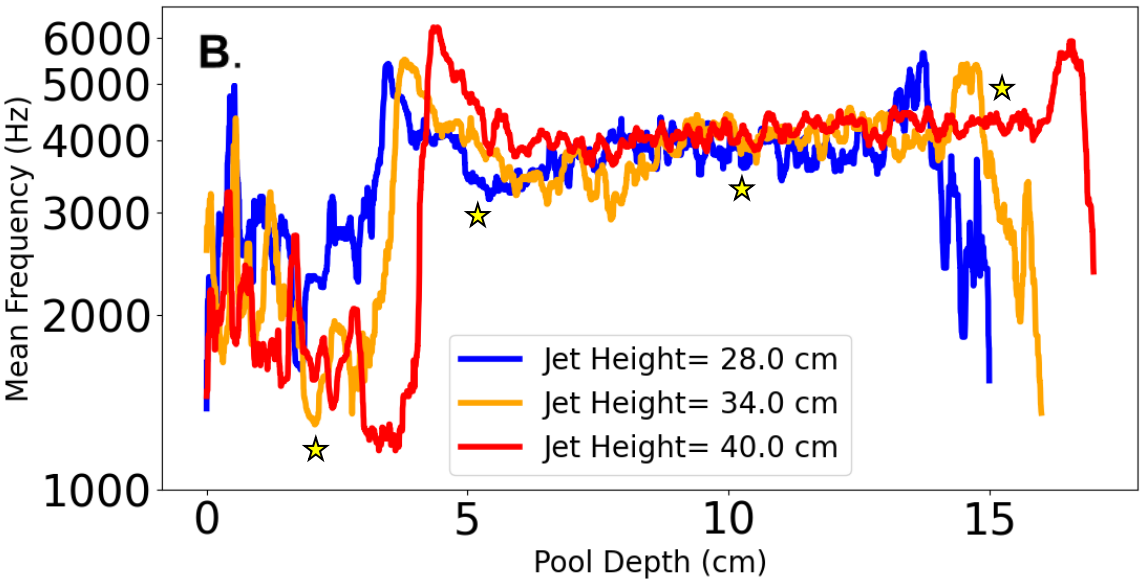
B.
6000
5000
4000
3000
2000
1000
Mean Frequency (Hz)
0
5
10
15
Pool Depth (cm)
Jet Height= 28.0 cm
Jet Height= 34.0 cm
Jet Height= 40.0 cm

Figure 2.9. Power [A] and Mean Frequency [B] as a function of tailwater pool depth for three jet heights. Yellow stars represent the pool depths photographed in Figure 8.

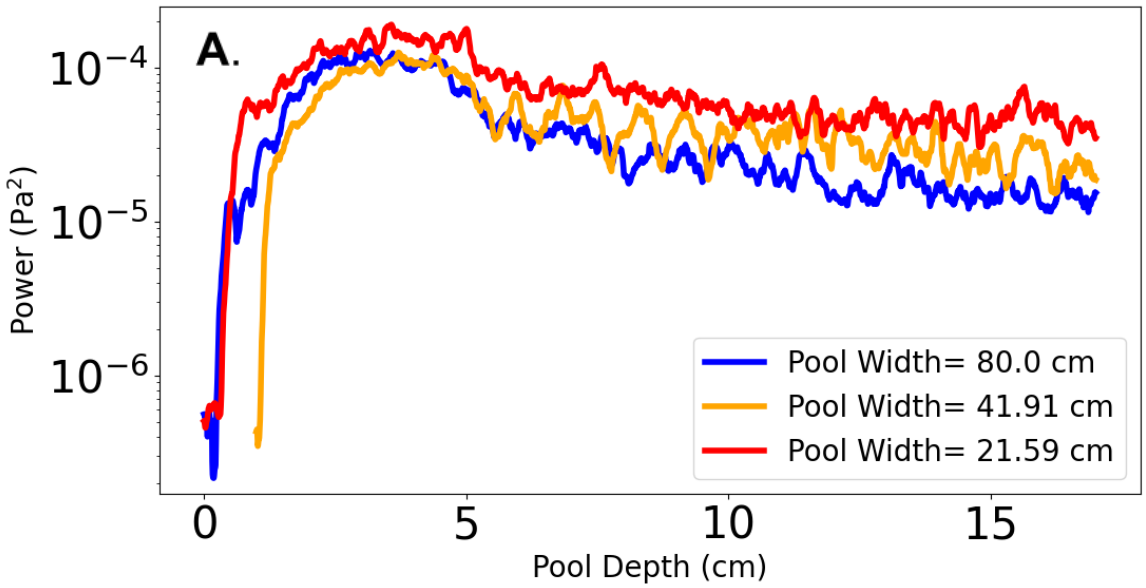

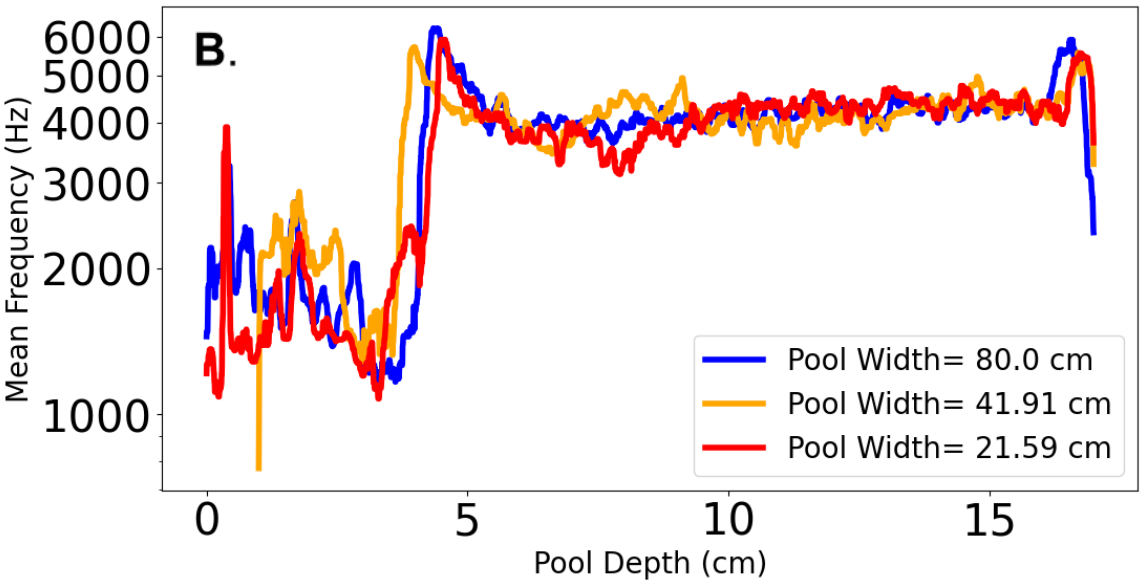

Figure 2.10. Power [A] and Mean Frequency [B] as a function of tailwater pool depth for three pool widths.

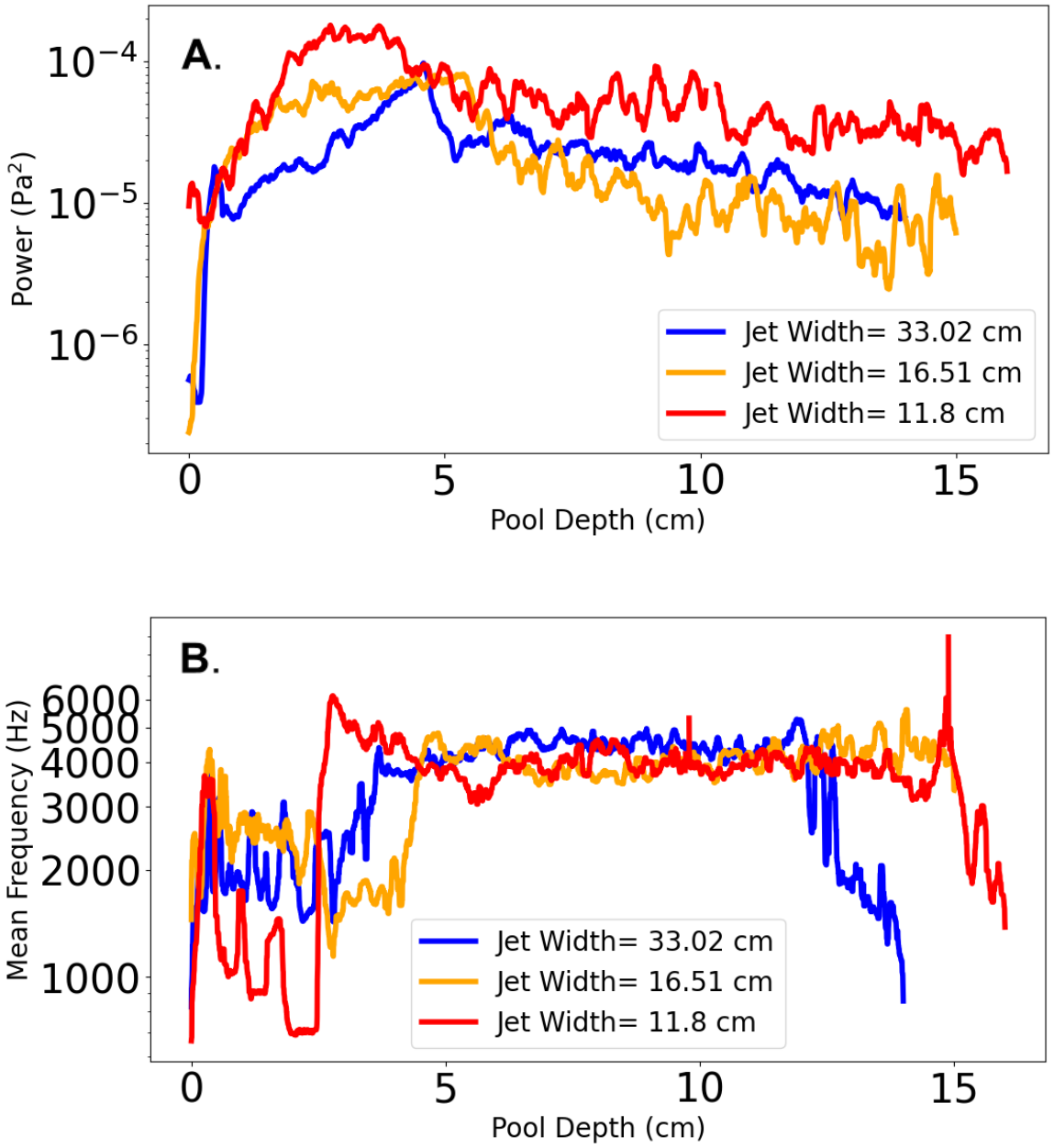

Figure 2.11. Power [A] and Mean Frequency [B] as a function of tailwater pool depth for three jet widths.

We see clear effects of both jet height and pool width on our recordings. As jet height increases, we observe higher power at all pool depths (Figure 9 A). Mean

frequency reaches a lower minimum and higher maximum value as jet height increases, and transitions in mean frequency occur at greater pool depths (Figure 9 B). We also see a trend in pool widths where the smallest pool width produced the highest power consistently while the larger pools decreased power (Figure 10 A). Mean frequency is consistent among pool width variations (Figure 10 B).

Much of the variation of the recorded signals in the jet width experiment was difficult to explain as a simple dependence on jet width. At the smallest jet width, power is loudest for the entirety of the recording (Figure 11 A). As jet width increases, we observe a decrease in power at shallow depths, but no trend past ~5 cm. Mean frequency spans the largest range at the smallest jet width but displays no other trends at greater jet widths (Figure 11 B).

For the jet height scenario, power slowly decreases, and oscillations are small at pool depths > 5 cm (Figure 9 A). The jet width and pool width scenarios produce two recordings where oscillations are large at depths > 5 cm, and one recording where oscillations are smaller. Mean frequency varies greatest at the jet width scenario, followed by the jet height scenario, and finally the pool width scenario.

2.4. Discussion

2.4.1 Morphological Effects on Acoustics

The plunge-pool experiment demonstrates the dependence of acoustic power and mean frequency on jet and pool morphologies at vertically stepped plunge-pool features (Figures 9-11). Submergence, where steps are less effective as energy dissipators, is used to describe the point where vertical fall is less pronounced or no longer present at a plunge-pool (Chin, 2003). Submergence represents a significant, discrete morphological change in flow structure that may explain observed acoustic tendencies.

Every iteration of the plunge-pool experiment reveals an initial rise and eventual fall in acoustic power despite constant discharge at variable pool depth (Figures 9-11). For eight of nine model iterations, mean frequency also rises and eventually falls. At stepped, plunge-pool-like Boise River features, a similar oscillation in both power and frequency is observed (Figure 6 A). This experiment offers variable pool depth and flow structure as possible explanations for acoustic variance with discharge. Pool depth increasing impairs the effectiveness of energy reduction by steps; they are most effective at reducing stream energy at low stage and their effectiveness falls with greater stage (Chin, 2003). Since we also see acoustic power decreasing at high stages, when steps are expected to be less effective energy dissipators, we conclude that acoustic power can be a useful indicator of hydraulic power dissipation.

In the jet height experiment, we observed greater power and a shift in mean frequency between each increase in jet height (Figure 9). Observed acoustic power variability between jet height iterations may be a result of the jet impacting the pool with

greater energy when plunging from greater heights due to potential energy increases (Chanson & Manasseh, 2003; Pagliara et al. 2007). The mean frequency transition delays observed between jet height iterations suggest that mean frequency is partially controlled by flow structure and energy density (Pagliara et al., 2007). The power and frequency trends may also be a result of an increase in air entrainment rate (Chanson & Manasseh, 2003). Variability in free jet height and pool depth in natural fluvial settings occur when greater discharge increases the downstream depth of a step-like plunge-pool feature (Montgomery & Buffington, 1997; Pagliara et al., 2007; Scheingross & Lamb, 2016). Here, similar acoustic patterns to those in our jet height experiment may be observed.

In the pool width experiment, we observed greater power and no shift in mean frequency between each decrease in pool width (Figure 10). The power variability between pool width iterations may be a result of jet energy density and flow constraint variations (Figure 10 A; Borghei & Zarnani, 2008). As pool width increases, flow is less geometrically constrained and jet energy has more room to disperse, causing less severe velocity gradients, less energy density, and therefore less acoustic power. The overall consistency of the mean frequency between iterations suggests that acoustic frequency is primarily controlled by the relationship between the jet morphology and the pool depth (Figure 10 B). In natural plunge-pool settings, pool width may change at higher stages or when significant bank erosion occurs (Montgomery & Buffington, 1997).

In the jet width experiment, we observed no overall trend in power or frequency, but the smallest jet width produced the greatest power and frequency range (Figure 11). Power variability between jet width iterations at shallow depths (0-5 cm) may be explained as variations in the downstream velocity component at the point of impact

(Figure 11 A). As jet width increases, specific discharge decreases, decreasing the downstream velocity component and the energy density of flow. Following the convergence of the powers at ~5 cm, the largest jet width's behavior appears to deviate from the expected trend. However, for depths >5 cm, differences in power and frequency cannot be explained as a simple monotone (where slope is positive everywhere or negative everywhere) dependence on jet width (unlike the pool width and jet height experiments). Due to small jet width/ pool width ratios for these iterations (< 0.41), our data may be insufficient to display a meaningful pattern. In addition, achieving precise similarity among plunging jet flows is challenging due to dynamic interactions between entrained bubbles and a developing mixing layer (Chanson & Manasseh, 2003). However, since the smallest jet width produces the loudest power and largest mean frequency variance, we suggest that jet width may partially control the acoustics at plunge-pools. Additional model runs with more data points are needed to better constrain the role of jet width on acoustics.

2.4.2 Discharge Effects on Acoustics

2.4.2.1. Flume Discharge Effects

At the morphologically constant, geometrically constrained flume plunge-pool the observed discharge-sound relationship is nonlinear, and non-monotone (Figure 3; Figure 4). Namely, from iterations 5-7 infrasound power increases by 0.5% then decreases while discharge increases by 9% at each iteration. Simultaneously, audible sound power increases by 5% then negligibly decreases. Audible and infrasound power's behavior from iterations 5-7 may be explained by flow reaching a physical limit where it cannot

expand further downstream or underwater. Audible mean frequency decreases continuously until reaching iterations 5-7, where it begins to increase. Infrasound mean frequency trends change several times, with major changes occurring at iterations 1, 3, and 5. Audible and infrasound power and audible mean frequency appear to suggest a change in flow behavior from iterations 5-7 (Figure 4).

2.4.2.2. Riffle Discharge Effects

At both riffle and step-like features at field sites, discharge-sound relationships are nonlinear, non-monotone, and depend on channel size and feature morphology (Figure 5-7). Despite these complexities, acoustic rating curves at some sites may be developed to predict discharge from a recording of sound.

FB5 riffle increases in power while increasing then decreasing in mean frequency, while FB1 riffle decreases in power while decreasing then increasing in mean frequency (Figure 5). These conflicting patterns observed at Boise River riffles suggest that low slope features in pool-riffle channels produce variable flow structures at a range of discharges due to irregular, possibly vertically and laterally oscillating bedforms (Montgomery & Buffington., 1997). Changes in discharge may be causing the submergence of sound sources at FB1, and the emergence or migration of them at FB5. Primary resistance to flow at pool-riffle reaches is drag from riffle-pool topographic roughness on the channel bed, therefore at higher discharges flow may be less affected by form roughness resulting in less noise generating whitewater at FB1 (Montgomery & Buffington, 1997). Conversely, increasing discharge at features with lateral or vertical

heterogeneity may result in the movement or genesis of whitewater sources at FB5, increasing its power.

2.4.2.3. Step Discharge Effects

The trend of Boise River step feature rating curves sharply increasing in power until reaching a threshold where power either falls or increases slowly with discharge agrees with our flume experiment data (Figure 6). The form of these curves, namely Settlers, also resemble those of the plunge-pool model runs (Figures 9-11). The power limit may be explained by the dependence of pool depth on discharge and, therefore, a submergence of whitewater at greater pool depths. This shortens the free jet height and limits the jet's impact velocity at a plunge-pool like step feature. The conflicting trends in mean frequency responses to discharge may be a result of human morphological intervention at configurable Diversion and Ridenbaugh dams. Although we did not observe frequent configuration changes when visiting these two features in the field, we acknowledge that these changes may affect acoustic signals. At Settlers, a non-adjustable low head dam, decreasing mean frequency with discharge agrees with our data from the flume experiment and with audible sound recorded from smaller features in DCEW. Power tracks discharge best at Diversion, a site with a large drop height (20 m) that is negligibly affected by changes in downstream pool depth. Mean frequency inversely tracks discharge best at Settlers, a site with constant morphology upstream of its flow receiving pool.

The increasing power and decreasing mean frequency with increasing discharge observed at two of three DCEW features suggest that stepped features with small W/D

ratios (< 5) are promising acoustic stream gauging sites (Figure 7). While audible data from LG step display an anomalously decreasing power and increasing mean frequency trend at DCEW, the large free jet height (~0.5 m) and observed strong correlation between infrasound power and discharge from 2021 suggest that dominant frequencies ~40 Hz may be more useful information at this site. As discharge increases, a greater pool depth and shorter free jet height submerging small bubbles at the surface is one explanation for the decreasing audible power at high discharges. LG's morphology may be qualitatively described as a step-pool (Montgomery & Buffington., 1997) feature whose steps often submerge at high discharges and dissipate energy less effectively (Chin, 2003). The monotonic form of both the power and mean frequency rating curves at CON1E and CON1W show that these sites are the most successful of all study sites at estimating discharge (Figure 7). CON1W and CON1E consist of steeply sloped channels with many sound sources, making them robust areas for acoustic stream gauging.

2.4.2.4. Acoustic Model Curves

Using one variable as a proxy for another (in this case, sound characteristics for discharge) works best when the relationship between the variables is monotone (and therefore unambiguous) and strong (low degree of scatter). At all Boise River sites, we observe a higher amount of power and frequency scatter at relatively low discharges of ~10-20 m^3/s than at higher discharge. At LG and CON1E, mean frequency plots have a higher amount of scatter at lower discharges than at high discharge. Conversely, at LG the greatest amount of power scatter is at low discharges, while at CON1E there is more scatter at high discharges. CON1W displays data with the least amount of scatter for both power and frequency and will therefore estimate discharge with greatest certainty among

the sites studied. For all step features, model curves change their respective trends at certain discharge thresholds (Figures 5-7). A high amount of scatter or a changing trend within a model curve may be due to morphological inconsistencies in the channel, shifting overall flow structure (Osborne et al., 2021). At low discharges, high scatter could be a result of low signal to noise ratios. We conclude that step-like features with a dense concentration of sound sources in channels with small W/D ratios tend to be the most promising candidates for acoustic gauging, and steps with large drop heights and W/D ratios are also favorable. The ability to use both power and mean frequency to estimate discharge is a potential advantage acoustic model curves have over stage-only curves, as acoustic signals contain more information on how a river reach may be changing.

2.5. Conclusion

While past research has evaluated the effects of discharge and flow morphology on acoustic signals separately in either field or laboratory settings, this study investigates these variables jointly in natural, dam regulated, and laboratory fluvial settings. To elucidate the roles of discharge and flow morphology on acoustic signals, this study examined sound from eight stream-gauged, morphologically diverse study sites, a discharge-variable morphologically constant flume plunge-pool, and a morphologically variable discharge-constant plunge-pool. Rising downstream depth at a plunge-pool strongly influences both acoustic power and frequency. The initial drop height of a plunging jet and the width of its receiving pool were found to clearly influence acoustic signals, while the width of a plunging jet may also play a role in acoustics. Using sound to infer discharge works well at step features with low W/D ratios, at high W/D ratio step

features with negligibly changing morphologies, and sometimes works at riffle features and morphologically variable step features. At several field sites, we observed power to increase with discharge until a certain threshold, where it either does not change or decreases with rising discharge. With more studies in morphologically diverse channels such as bedrock and cascade, acoustics may be used as a non-invasive, inexpensive, and accurate hydrometric tool.

This study finds that a whitewater feature's morphology and discharge strongly affect the recorded fluvial acoustic signals. At plunge-pool-like features, sound power and frequency are strongly affected by the morphologies of the plunging jet and its receiving pool. This dependence may explain power and frequency oscillations at Boise River and DCEW plunge-pool-like features. At both riffle and step-like field site features, discharge-sound relationships are nonlinear, non-monotone, and depend on channel size and feature morphology. The trend of the Boise River step rating curves sharply increasing in power until reaching a threshold where power either falls or increases slightly with increasing discharge agrees with data from the plunge-pool and flume experiments. The trends observed at DCEW steps are similar, but we don't observe a decreasing power trend with increasing discharge possibly due to discharge not reaching a threshold that submerges whitewater during the study period. The trend of step features with small W/D ratios increasing in power and decreasing in frequency with increasing discharge is consistent with Boyd & Varley, 2004 which attributed increasing bubble sizes from higher velocity plunging jet flows as a lower frequency, higher amplitude underwater acoustic signal. Simultaneously increasing power and decreasing frequency is also observed at shallow depths (< 5 cm) during the plunge-pool experiment. The

contrasting trends of the Boise River riffles indicate that riffles at flows with large W/D ratios may not be useful sites for acoustic stream gauging. We conclude that acoustic stream gauging has potential at large step features with a stable relationship between feature height and tailwater pool depth, and at small step features with a high concentration of whitewater sound sources.

Although sound power changes predictably with discharge at several fluvial features observed (Figure 12), calibration is still needed. Acoustic stream gauging does not fully solve a key problem stage-based gauging has, the need for invasive calibration, but with calibration it is still less invasive than stage-based gauging. Acoustic stream gauging may be most useful at high gradient and discharge, small channeled fluvial systems which are difficult or impractical to access directly for measurements. It may also be useful to complement or verify depth-based stream gauges or remote sensing data, and to address hydrologic monitoring gaps for low-order streams and other under-monitored systems. Further acoustic studies are needed in fluvial systems with morphologically resistant bedrock, and at different discharge and channel scales compared to those observed in this study.

Site	Power trend	Frequency trend	Power uncertainty	Frequency uncertainty
FB1 riffle (Boise River)	2	1	High	Medium
FB5 riffle (Boise River)	3	1	High	High
Settlers step (Boise River)	2	3	Low	Low
Ridenbaugh step (Boise River)	1	1	Medium	Low
Diversion step (Boise River)	3	1	Low	Medium
LG step (DCEW)	3	1	High	Low
CON1E step (DCEW)	3	2	Medium	High
CON1W step (DCEW)	3	3	Low	Low

Figure 2.12. A table ranking the rating curve trends and qualitatively defined uncertainty for each acoustic variable at each site. Trends are scored according to: 3: Trend is monotonic over measured discharge range. 2: Trend is non-monotonic but remains consistent (power or frequency is relatively predictable for a given discharge). 1: Trend is overall inconsistent and difficult to predict. Uncertainties are classified as either high, medium, or low based on the deviation of data from the trend line of fit. CON1W, Settlers, and Diversion are in the top tier among study sites, followed by CON1E and LG in the middle tier, and FB1, FB5, and Ridenbaugh in the low tier.

REFERENCES

Anderson, J. F., Johnson, J. B., Bowman, D. C., & Ronan, T. J. (2018). The Gem infrasound logger and custom-built instrumentation. Seismological Research Letters, 89(1), 153-164.

Borghei, S. M., & Zarnani, P. (2008). Jet impact geometry and plunge pool dimensions effects on dynamic pressures at pool sidewalls. Canadian Journal of Civil Engineering, 35(4), 408–417. https://doi.org/10.1139/L07-141

Boyd, J. W. R., & Varley, J. (2004). Acoustic emission measurement of low velocity plunging jets to monitor bubble size. Chemical Engineering Journal, 97(1), 11–25. https://doi.org/10.1016/S1385-8947(03)00115-3

Buchanan, T. J., Somers, W. P., & Survey, U. S. G. (1976). Discharge measurements at gaging stations. Techniques of Water-Resources Investigation, Book 3, Chapter A8, 65.

Chachereau, Y., & Chanson, H. (2011). Free-surface fluctuations and turbulence in hydraulic jumps. Experimental Thermal and Fluid Science, 35(6), 896–909. https://doi.org/10.1016/j.expthermflusci.2011.01.00

Chacon-Hurtado, J. C., Alfonso, L., & Solomatine, D. P. (2017). Rainfall and streamflow sensor network design: A review of applications, classification, and a proposed framework. Hydrology and Earth System Sciences, 21(6), 3071–3091. https://doi.org/10.5194/hess-21-3071-2017

Chanson, H., & Manasseh, R. (2003). Air Entrainment Processes in a Circular Plunging Jet: Void-Fraction and Acoustic Measurements. Journal of Fluids Engineering, Transactions of the ASME, 125(5), 910–921. https://doi.org/10.1115/1.1595672

Chin, A. (2003). The geomorphic significance of step-pools in mountain streams. Geomorphology, 55(1–4), 125–137. https://doi.org/10.1016/S0169-555X(03)00136-3

Chow, V. Te. (2007). Open-channel hydraulics, McGraw-Hill civil engineering series Civil Engineering Series. 680.

McNamara, James, Boise State University. (2017) Long-term hydrometeorologic data time series, 1998-present, Dry Creek Experimental Watershed, Southwest Idaho. https://doi.org/10.18122/B2VG6G

Evans, G. M., Jameson, G. J., & Rielly, C. D. (1996). Free jet expansion and gas entrainment characteristics of a plunging liquid jet Experimental Thermal and Fluid Science, 12(2), 142–149. https://doi.org/10.1016/0894-1777(95)00095-X

Gimbert, F., Tsai, V. C., & Lamb, M. P. (2014). A physical model for seismic noise generation by turbulent flow in rivers. Journal of Geophysical Research: Earth Surface, 119(10), 2209–2238. https://doi.org/10.1002/2014JF003201

Hannah, D. M., Demuth, S., van Lanen, H. A. J., Looser, U., Prudhomme, C., Rees, G., Stahl, K., & Tallaksen, L. M. (2011). Large-scale river flow archives: Importance, current status and future needs. Hydrological Processes, 25(7), 1191–1200. https://doi.org/10.1002/hyp.7794

Hill, A. P., Prince, P., Snaddon, J. L., Doncaster, C. P., & Rogers, A. (2019). AudioMoth: A low-cost acoustic device for monitoring biodiversity and the environment. HardwareX, 6, e00073. https://doi.org/10.1016/j.ohx.2019.e00073

Hsu, L., Finnegan, N. J., & Brodsky, E. E. (2011). A seismic signature of river bedload transport during storm events. Geophysical Research Letters, 38, L13407. https://doi.org/10.1029/2011GL047759

Krabbenhoft, C. A., Allen, G. H., Lin, P., Godsey, S. E., Allen, D. C., Burrows, R. M., DelVecchia, A. G., Fritz, K. M., Shanafield, M., Burgin, A. J., Zimmer, M. A., Datry, T., Dodds, W. K., Jones, C. N., Mims, M. C., Franklin, C., Hammond, J. C., Zipper, S., Ward, A. S., … Olden, J. D. (2022). Assessing placement bias of the global river gauge network. Nature Sustainability, 0–13. https://doi.org/10.1038/s41893-022-00873-0

Le Guern, J., Rodrigues, S., Geay, T., Zanker, S., Alexandre Hauet, Tassi, P., Claude, N., Philippe Jugé, Duperray, A., & Vervynck, L. (2020). *Relevance of acoustic methods to quantify bedload transport and bedform dynamics in large sandy-gravel bed river*. Earth Surface Dynamics. https://doi.org/10.5194/esurf-2020-77

Lyons, J. J., Dietterich, H. R., Patrick, M. P., & Fee, D. (2021). High-speed lava flow infrasound from Kīlauea's fissure 8 and its utility in monitoring effusion rate. Bulletin of Volcanology, 83(11). https://doi.org/10.1007/s00445-021-01488-7

Mao, L., Carrillo, R., Escauriaza, C., & Iroume, A. (2016). Flume and field-based calibration of surrogate sensors for monitoring bedload transport. Geomorphology, 253, 10–21. https://doi.org/10.1016/j.geomorph.2015.10.002

Marineau, Mathieu, Wright, Scott, Gaeuman, David, Curran, Chris, Stark, Kyle, Siemion, Jason, Schenk, Edward (2019). Overview of Five Recent Bedload Monitoring Field Experiments Using Hydrophones. U.S.Geologic Survey.

Montgomery, D. R., & Buffington, J. M. (1997). Channel-reach morphology in mountain drainage basins. Bulletin of the Geological Society of America, 109(5), 596–611. https://doi.org/10.1130/0016-7606(1997)109<0596:CRMIMD>2.3.CO;2

Mossa, M. (1999). On the oscillating characteristics of hydraulic jumps. Journal of Hydraulic Research, 37(4), 541–558. https://doi.org/10.1080/00221686.1999.9628267

Odzer, M., & Francke, K. (2020). Acoustic study of wave-breaking to enhance the understanding of wave physics. Proceedings of the International Conference on Offshore Mechanics and Arctic Engineering - OMAE, 6B-2020, 1–6. https://doi.org/10.1115/omae2020-19352

Osborne, W. A., Hodge, R. A., Love, G. D., Hawkin, P., & Hawkin, R. E. (2021). Babbling brook to thunderous torrent: Using sound to monitor river stage. Earth Surface Processes and Landforms, 46(13), 2656–2670. https://doi.org/10.1002/esp.5199

Pagliara, S., Amidei, M., & Hager, W. H. (2008). Hydraulics of 3D Plunge Pool Scour. Journal of Hydraulic Engineering, 134(9), 1275–1284. https://doi.org/10.1061/(asce)0733-9429(2008)134:9(1275)

Park, J., Garcés, M., Fee, D., & Pawlak, G. (2008). Collective bubble oscillations as a component of surf infrasound. The Journal of the Acoustical Society of America, 123(5), 2506–2512. https://doi.org/10.1121/1.2885743

Petrut, T., Geay, T., Gervaise, C., Belleudy, P., & Zanker, S. (2018). Passive acoustic measurement of bedload grain size distribution using self-generated noise. *Hydrology and Earth System Sciences*, *22*(1), 767–787. https://doi.org/10.5194/hess-22-767-2018

Podolskiy, E. A., Imazu, T., & Sugiyama, S. (2023). Acoustic sensing of glacial discharge in Greenland. *Geophysical Research Letters*, 50, e2023GL103235. https://doi.org/10.1029/2023GL103235

Richardson, R., Guilinger, J. (2015). Geomorphic Assessment of the Lower Boise River, Idaho. Technical Report. Accessed February 2023 at URL http://www.boiseriverenhancement.org/wp-content/uploads/2016/09/LowerBoise_GeomorphAssess_RichardsonGuilinger_BOR_2015.pdf

Ronan, T. J., Lees, J. M., Mikesell, T. D., Anderson, J. F., & Johnson, J. B. (2017). Acoustic and Seismic Fields of Hydraulic Jumps at Varying Froude Numbers. Geophysical Research Letters, 44(19), 9734–9741. https://doi.org/10.1002/2017GL074511

Scheingross, J. S., & Lamb, M. P. (2016). Sediment transport through self-adjusting, bedrock-walled waterfall plunge pools. Journal of Geophysical Research: Earth Surface, 121(5), 939–963. https://doi.org/10.1002/2015JF003620

Schmandt, B., Aster, R. C., Scherler, D., Tsai, V. C., & Karlstrom, K. (2013). Multiple fluvial processes detected by riverside seismic and infrasound monitoring of a controlled flood in the Grand Canyon. Geophysical Research Letters, 40(18), 4858–4863. https://doi.org/10.1002/grl.50953

Slad, G. W., & Merchant, B. J. (2016). Chaparral Model 60 infrasound sensor evaluation. Technical Report, March, SAND2016--1902.

Tsai, V. C., Minchew, B., Lamb, M. P., & Ampuero, J.-P. (2012). A physical model for seismic noise generation from sediment transport in rivers. Geophysical Research Letters, 39, L02404. https://doi.org/10.1029/2011GL050255

U.S. Geological Survey, (2021, 2022), National Water Information System data available on the World Wide Web (USGS Water Data for the Nation), accessed September 2022, at URL https://waterdata.usgs.gov/monitoring-location/13206000/#parameterCode=00060&startDT=2021-03-12&endDT=2022-10-15.